

# Three Orbital Burns to Molniya Orbit via Shuttle/Centaur G Upper Stage

Craig H. Williams<sup>1</sup>

NASA Glenn Research Center, Cleveland, OH 44135

An unclassified analytical trajectory design, performance, and mission study was done for the 1982-86 joint NASA-USAF Shuttle/Centaur G upper stage development program to send performance-demanding payloads to high orbits such as Molniya using an unconventional orbit transfer. This optimized three orbital burn transfer to Molniya orbit was compared to the then-baselined two burn transfer. The results of the three dimensional trajectory optimization performed include powered phase steering data and coast phase orbital element data. Time derivatives of the orbital elements as functions of thrust components were evaluated and used to explain the optimization's solution. Vehicle performance as a function of parking orbit inclination was given. Performance and orbital element data was provided for launch windows as functions of launch time. Ground track data was given for all burns and coasts including variation within the launch window. It was found that a Centaur with fully loaded propellant tanks could be flown from a 37° inclination low Earth parking orbit and achieve Molniya orbit with comparable performance to the baselined transfer which started from a 57° inclined orbit: 9,545 lb vs. 9,552 lb of separated spacecraft weight respectively. There was a significant reduction in the need for propellant launch time reserve for a one hour window: only 78 lb for the three burn transfer vs. 320 lb for the two burn transfer. Conversely, this also meant that longer launch windows over more orbital revolutions could be done for the same amount of propellant reserve. There was no practical difference in ground tracking station or airborne assets needed to secure telemetric data, even though the geometric locations of the burns varied considerably. There was a significant adverse increase in total mission elapsed time for the three vs. two burn transfer (12 vs. 1¼ hrs), but could be accommodated by modest modifications to Centaur systems. Future applications were discussed. The three burn transfer was found to be a viable, arguably preferable, alternative to the two burn transfer.

## Nomenclature

$a$	= semi-major axis
$C3$	= orbital energy per unit mass (from Newton's "vis viva" equation)
$e$	= eccentricity
$i$	= inclination
$L$	= mass ratio
$l$	= semi latus rectum
$M$	= mass
$N$	= angle of perturbing thrust, in orbital plane, normal to motion
$R$	= radius
$r$	= radius of instantaneous position
$T$	= angle of perturbing thrust, in orbital plane, tangent to motion
$t$	= time
$u$	= argument of the latitude ( $\theta + \omega$ )
$V$	= velocity
$W$	= angle of perturbing thrust, normal orbital plane, positive where acceleration is positive
$\Delta$	= change

---

<sup>1</sup> Aerospace Engineer, NASA Glenn Research Center, Propulsion Division, MS 142-5, 21000 Brookpark Rd., Cleveland, OH, 44135, Associate Fellow AIAA.

$\theta$	= true anomaly
$\mu$	= product of Gravitational constant and mass of Earth = 62,748.55 nmi <sup>3</sup> /sec <sup>2</sup>
$\Omega$	= node
$\omega$	= argument of the perigee

#### Subscripts

2	= Burn 2
3	= Burn 3
<i>a</i>	= apogee
<i>D1</i>	= coast 1 drop mass
<i>D2</i>	= coast 2 drop mass
<i>max</i>	= maximum
<i>p</i>	= perigee
<i>PL</i>	= payload
<i>prop</i>	= propellant
<i>T</i>	= total

## I. Introduction

An unclassified analytical trajectory design, performance, and mission analysis study was done for the 1982-86 Joint National Aeronautics and Space Administration (NASA) – United States Air Force (USAF) Shuttle/Centaur G upper stage development program to send performance-demanding payloads to high orbits such as Molniya. Motivated to mitigate a major concern at that time pertaining to the deployment of a significantly off-loaded Centaur stage from the Shuttle cargo bay, this orbital transfer method offered the potential to fill Centaur propellant tanks and secure comparable (or superior) performance compared to the baselined two burn transfer.

The Shuttle/Centaur upper stage development program of the 1980's was to produce the highest performing upper stages of that time. While the program produced two flight articles and was less than four months of launch, it (like many space systems) was a casualty of the repercussions of the Challenger Space/Shuttle accident of January 1986. Like many of the accomplishments of a fast moving space development and operational program, there was insufficient time to document noteworthy technical work. Following its cancellation, many of these achievements were left undocumented. During this fiftieth anniversary of the Centaur upper stage, this paper is an attempt to remedy one of these many achievements: the validation of a three orbital burns to Molniya orbit solution via Shuttle/Centaur G upper stage. Because of the unusual trajectory design and orbital mechanics involved, this subject could be of interest not just for historical reasons, but possible application to future launch vehicles as well.

## II. Background

### A. Shuttle/Centaur G Upper Stage and its Missions

Shuttle/Centaur was a joint NASA & USAF upper stage development program initiated in July 1982 (with some early work in 1981). Based on the existing, highly successful Atlas/Centaur upper stage, Shuttle/Centaur was to be an expendable system (with its origin in unmanned space system) used by the partially reusable Space Shuttle system (a manned space system).<sup>1</sup> This was to be another successful teaming of experienced expendable launch vehicle development organizations: NASA Lewis Research Center (LeRC), USAF/Aerospace Corporation, and General Dynamics Corporation. This government & industry team developed two versions of Shuttle/Centaur upper stages: the smaller "G" version primarily for national security missions and the larger "G-Prime" version designed primarily for NASA interplanetary missions. Compared to other launch vehicles at the time, Shuttle/Centaur represented a doubling of performance capability for comparable missions. A joint program office was established at Cleveland's NASA LeRC with a co-located USAF Space Division detachment. The same Atlas/Centaur major contractors were retained: General Dynamics (Centaur stage), Pratt & Whitney (RL10 engines), Teledyne (Digital Computer Unit and other avionics), and Honeywell (Inertial Navigation Unit and other avionics).<sup>2</sup>

Shuttle/Centaur G and its payload were to be cradled by the Centaur Integrated Support System (CISS) within the Shuttle cargo bay. The CISS and the forward attach points supported the upper stage and payload from Space Shuttle mating through cargo bay deployment on-orbit. Once in orbit, with cargo bay doors opened, the CISS rotated the Centaur/payload to the deployment angle and the Centaur/payload were deployed. Figure 1 is an artist's conception of a Shuttle/Centaur G and payload in low Earth orbit following deployment from the Space Shuttle's cargo bay. Shuttle/Centaur would then maneuver to a predetermined safe location, fire its engines, and inject the

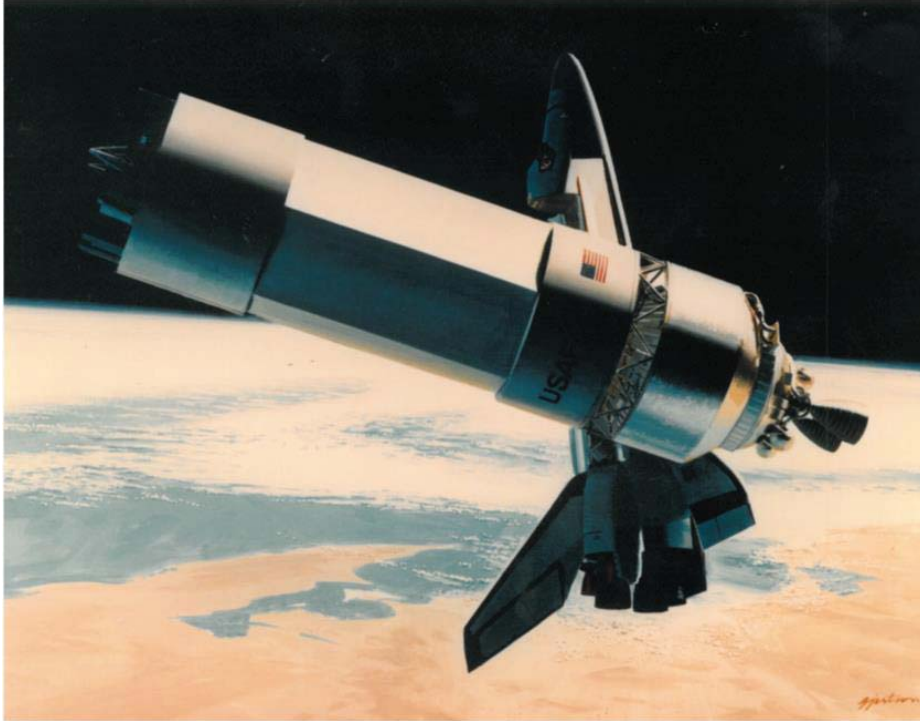


**Figure 1. Artist's View of Deployed Shuttle/Centaur G with Payload.**

spacecraft to the desired orbit. The first two missions (each using the G-Prime version) were the Galileo mission to Jupiter and the International Solar Polar Mission (re-named Ulysses) to the sun. Both missions were slated for launch within days of each other in May 1986.

The Shuttle/Centaur program made rapid progress. Within 3½ years following authority to proceed, two G-Prime flight vehicles had been designed, developed, manufactured, tested, integrated, and were being prepared for launch at the Cape. A pathfinder test article had also been built and preceded them. In addition, two G flight vehicles were approximately 50% complete by that same

time. Figure 2 illustrates the G-Prime rollout at the General Dynamics plant in Kearny Mesa, California in 1985.

Despite the cancellation of the Shuttle/Centaur program following the Space Shuttle Challenger disaster in 1986, the Shuttle/Centaur G-Prime vehicle was quickly adopted by the USAF/Space Division and integrated with its new Titan IV booster. From 1994 through 2003, the Titan IV/Centaur was launched 16 times: 14 were successful, one experienced a Centaur failure, and one experienced a Titan IV core failure (i.e. Centaur no-trial). One of the Titan IV/Centaur missions was the 1997 launch of the Cassini spacecraft to Saturn. This was NASA LeRC's last launch, ending its 35 year tenure leading NASA's expendable launch vehicle program. Shuttle/Centaur G-Prime (integrated with the Titan IV) remains to this day the last launch vehicle NASA has developed, integrated, and launched successfully.



**Figure 2. Shuttle/Centaur G-Prime Rollout at General Dynamics in 1985.**

Data from unclassified publications<sup>3, 4, 5, 6, 7</sup> of the time describe the vehicle system and performance used to model the

Shuttle/Centaur G vehicle system and the two 'generic' missions to which its performance was measured against. One of these was the 12 hour Molniya orbit --- an orbit which provided long (~ 10 hours) dwell times over a land mass. Shuttle/Centaur G's performance requirement to a generic Molniya orbit was 11,500 lbs. Another major requirement was to accommodate a 40 foot long payload within the existing 60 foot long Shuttle cargo bay. This requirement was the primary reason for the ten foot shorter G version (compared to the longer G-Prime). The drawing in Fig. 3 compares the G & G-Prime vehicles. The G's shorter, smaller tanks could only accommodate a nominal 30,000 lb propellant load (compared to the G-Prime's nominal 45,000 lb). This meant that a new version of the RL10 engine was needed to burn the propellants at a 6:1 mixture ratio rather than the heretofore standard of 5:1.

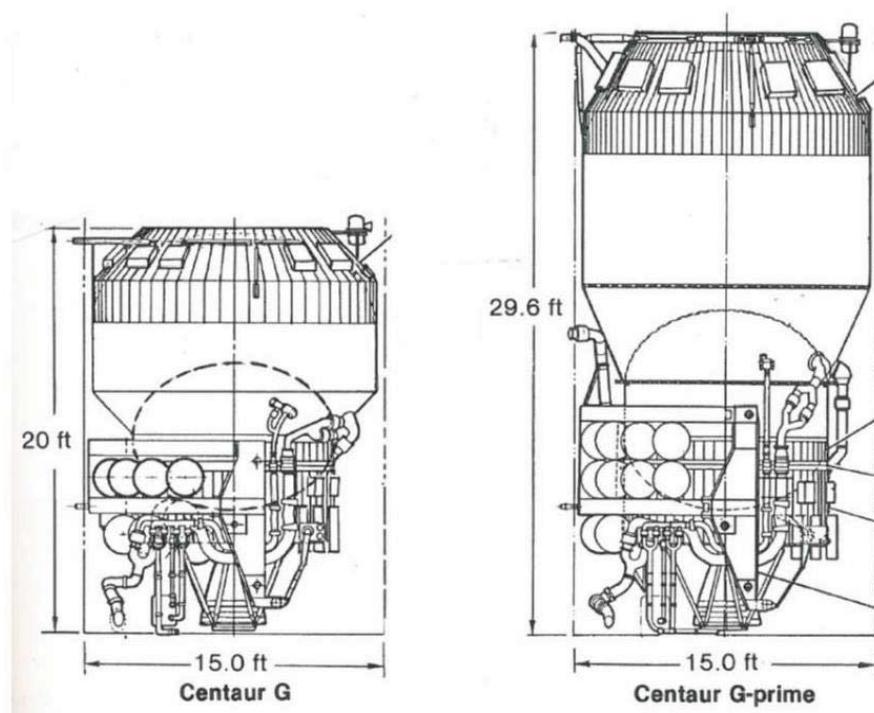


**Figure 3. Comparison of Shuttle/Centaur G and G Prime.**

## **B. Problem Statement**

Like all launch vehicles, the Space Shuttle lift capability was degraded as its launch azimuth (LAZ) was decreased from 90° due East. This was because as LAZ was lowered to increase the parking orbit inclination (assuming planar ascent), the smaller became the useful component of Earth's rotational velocity to achieve orbit, thus the lower the payload capability. In order to maximize payload to Molniya orbit, the lowest LAZ available from NASA's Kennedy Space Center (35°) was used for planar ascent to reach the maximum parking orbit inclination (57°). While this minimized the amount of plane change performed by the upper stage to reach the final 63.4° inclination Molniya orbit, it also severely reduced the Shuttle lift commitment by 16,600 lbs. This decrease in Shuttle capability forced a severe (~ 40 % by weight) offload of Centaur's total tankable propellants, resulting in a tremendous performance hit for the launch system.

This considerable off-load of Centaur propellants raised three major concerns for the mission planners:

--- The possibility of large scale dynamic instabilities associated with deploying a considerably offloaded Centaur due to unsettled propellants "sloshing" in the tanks could have led to an unstable deployment, and possibly a dangerous re-contact with the Space Shuttle. There was a strong desire to find a way to reduce the propellant off-load (i.e. fill the tanks) to ameliorate the problem, and also preclude the need to add slosh baffles which would increase dry weight. But an alternate approach implied a greater LAZ (to enable a greater Shuttle cargo element weight limit). An alternate transfer could preclude a complicated analysis designed to determine where the propellants would be located in the tank prior to deployment. In addition, any analysis on a significantly offloaded tank might have been more severely affected by tanking dispersions or late deployment than a fully loaded mission. Thus a study was initiated to discover an alternate approach to mitigate this problem. This concern was the primary motivation for exploring alternate transfers to Molniya orbit.

--- Shuttle/Centaur's performance was significantly degraded due to the propellant offload. There was a strong interest to find an alternate trajectory to enable a greater payload to Molniya orbit.

--- Launch windows were expected to be costly in terms of propellant margins which would have to be held in reserve. This was due to the high inclination parking orbit and its performance cost for out of plane yaw steering needed to generate the windows. Contributing to this problem, deployment from the cargo bay could be delayed until the seventh revolution (or even later ('second day deployment')) due to the nature of Shuttle/Centaur space operations. If a way could be found to lessen the amount of out of plane (yaw) steering and accommodate multiple revolutions, a greater payload to final orbit should have been possible.

To address these three major concerns, four analyses were performed for the generic Molniya mission:

- Physics of an alternate transfer and comparison to the standard transfer
- Performance of both transfers for a range of park orbit inclinations
- Performance for launch windows up to 1½ hours and deployment revolutions 5, 6, and 7
- Ground tracks for nominal transfers and range of main burns throughout the launch windows

### C. Origins of the Three Orbital Burns to Molniya Orbit Solution

The generic Molniya orbit has an:

- 14,340 nmi semi-major axis (which dictates a 12-hour period)
- 500 nmi perigee radius altitude (alt) (which defines the highly eccentric orbit, providing long dwell times (~10 hrs) over a specified land area (centered about apogee))
- 63.4° inclination (which eliminates the precession of the line of apsides)
- 270° argument of the perigee (which positions the long dwell time over the greatest northern latitudes)

The baseline 2B transfer to Molniya orbit via Shuttle/Centaur G is illustrated in Fig. 4.

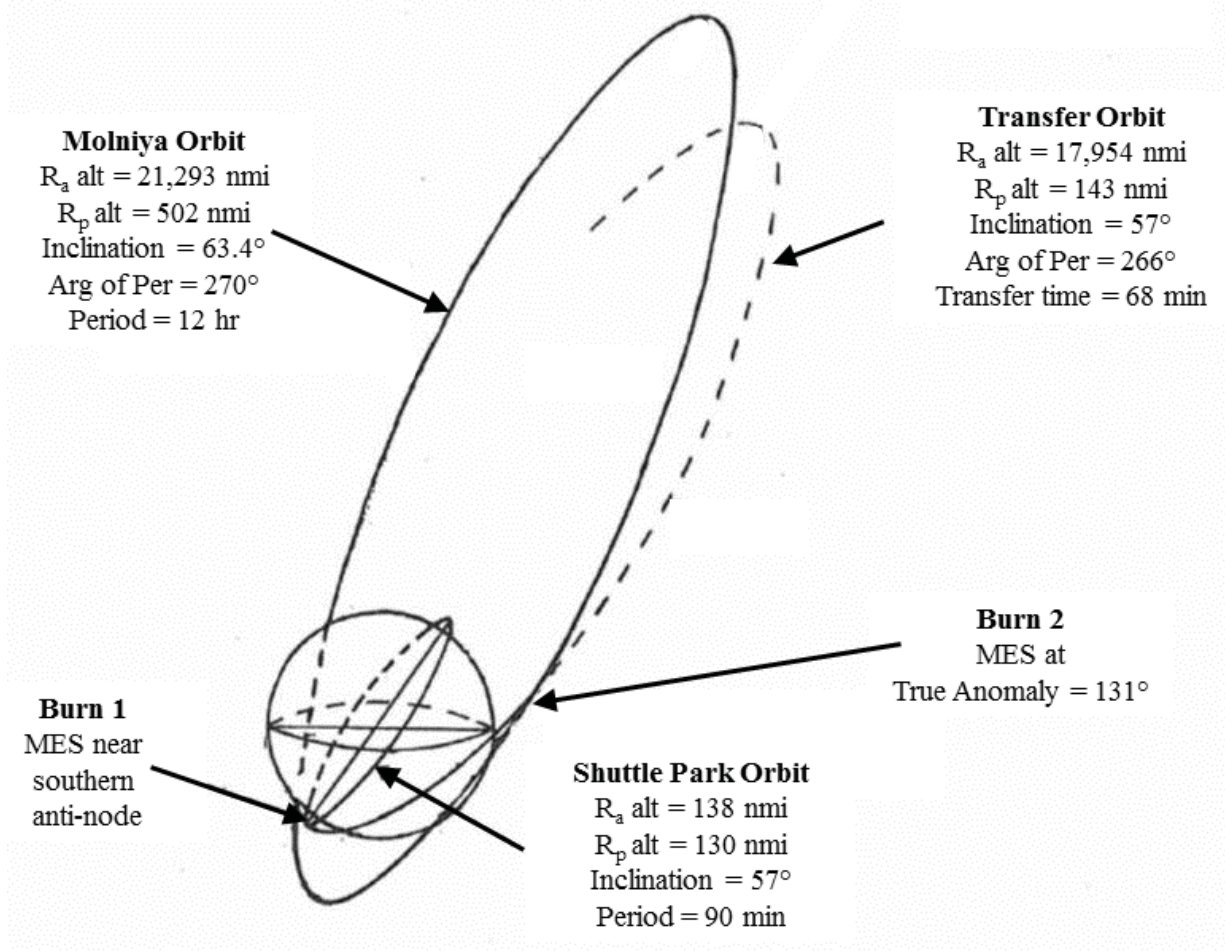


Figure 4. Two Burn Transfer to Molniya Orbit.

In the field of orbital mechanics and trajectory design, it is known that a class of optimal orbital transfers exist utilizing three burns (“3B”) following insertion into a low Earth parking orbit (LEO) for missions such as Molniya. While two orbital burn (“2B”) solutions are more conventional, 3B transfers have more degrees of freedom from which to yaw out of plane to satisfy requirements of angular orbital elements and enabling the possibility for greater performance. If a transfer could be found which started from a lower parking orbit inclination, a greater Shuttle lift capability could permit the filling of Centaur tanks. This would require Centaur to do more of the plane change, but a more efficient 3B transfer might enable a greater overall system performance.

The PhD thesis by Dr. Keith P. Zondervan of The Aerospace Corporation was used as the starting point for the baseline 3B trajectory for this analysis. Titled “Optimal Low Thrust, Three Burn Orbit Transfers with Large Plane Changes”, Dr. Zondervan’s thesis contained comprehensive material and detailed formulations of the optimal control and two point boundary value problems of orbital transfers.<sup>8</sup> The necessary conditions for the generalized problem were defined for both a “thrust-limited” case and an “acceleration-limited” case. Three methods of solving the two optimal control problems were given. The thesis worked through three lengthy example problems, each with a different initial and final orbit pair, and each with “thrust-limited” and “acceleration-limited” solutions. The examples also provided parametric data for various initial thrust-to-weight and final perigees. One of the comprehensive example problems was a 3B transfer from LEO to Molniya orbit.

The baseline 3B trajectory and transfer orbit characteristics for the Molniya transfer were obtained from the Zondervan thesis (“Aerospace solution”), and used as the target solution to converge to by the NASA analytical model. The specific Aerospace solution used was the example problem: inclination = 28.5° circular to 63.4° elliptic transfer (acceleration-limited solution) given in Tables 18 & 23 of the thesis. These data are for thrust to weight (T/W) of 1.0, which was equivalent to that of the Shuttle/Centaur G for the generic Molniya mission, except for  $R_p$  alt = 300 nmi. (Note: typographical errors exist in initial orbit inclination in Table 23 of Ref. 8.) Since no actual propulsion system was modeled in the thesis, the initial T/W and “acceleration-limited” relation served as proxies for the operational definition of the propulsive stage. The initial NASA analytic model (vehicle & trajectory) of the Shuttle/Centaur G was the existing high fidelity model for the generic 2B solution for a Molniya transfer. The model was created within NASA LeRC’s 3D computer program DUKSUP: a calculus of variations-based algorithm used to design high fidelity, optimized launch trajectories for Atlas/Centaur and Titan/Centaur vehicles for over 15 years.<sup>9, 10</sup> In order to first match the Aerospace solution, the “NASA GRC” model was simplified to eliminate detailed vehicle operation characteristics (such as hardware drops, propellant boiloffs/ventings/settlings, pre-chill/pre-start, and startup/shutdown transients). Then, the second burn was adjusted simultaneously as the third burn was introduced into the NASA GRC model. Gradually, the NASA GRC model was iterated to converge to the Aerospace solution of the three burn transfer.

Table 1 (columns 1& 2) contains the elements of the parking, transfer, and final orbits for both Aerospace and NASA GRC 3B baseline transfers, as well as the other data to be discussed in a later section. Consistent with other contemporary analytically modeled missions, a slightly elliptical parking orbit (160 X 148 nmi alt) was maintained in the NASA GRC model, where the Aerospace solution used a circular

**Table 1. Orbital Elements of Three and Two Burn Transfers.**

	3 Burn Aerospace PhD Thesis	3 Burn NASA GRC	3 Burn Aug 1984 mini-Colt	2 Burn Oct 1985 Colt
Parking orbit of period (hr)	1.5	1.5	1.5	1.5
Apogee altitude (nmi)	150.0	160.3	139.1	138.3
Perigee altitude (nmi)	150.0	147.7	130.4	130.4
Inclination (deg)	28.5	28.5	37.0	57.0
Argument of Perigee (deg)	0.0	206.8	3.4	-0.7
True Anomaly (deg)	0.0	36.1	-2.8	0.7
Node (deg)	0.0	189.4	189.7	2.0
Start 1st transfer orbit; coast duration (hr)	2.3	2.3	1.6	1.1
Apogee altitude (nmi)	20,355.7	20,403.8	17,059.4	17,953.8
Perigee altitude (nmi)	153.4	146.8	142.0	142.6
Inclination (deg)	29.1	29.1	37.5	57.0
Argument of Perigee (deg)	247.7	247.7	252.7	266.2
True Anomaly (deg)	6.9	7.0	10.5	8.2
Node (deg)	3.2	192.6	191.3	2.0
Start 2nd transfer orbit; coast duration (hr)	12.2	12.2	10.1	---
Apogee altitude (nmi)	26,550.9	26,556.5	23,115.8	---
Perigee altitude (nmi)	2,135.8	2,132.6	1,433.8	---
Inclination (deg)	57.4	57.4	58.3	---
Argument of Perigee (deg)	248.4	248.4	258.2	---
True Anomaly (deg)	133.0	133.0	127.4	---
Node (deg)	26.5	215.9	207.9	---
Molniya final orbit of period (hr)	12.0	12.0	12.0	12.0
Apogee altitude (nmi)	21,500.0	21,492.5	21,295.2	21,292.8
Perigee altitude (nmi)	300.0	299.9	504.9	502.1
Inclination (deg)	63.4	63.4	63.4	63.4
Argument of Perigee (deg)	270.0	270.0	270.0	270.0
True Anomaly (deg)	215.3	215.3	217.0	124.9
Node (deg)	15.7	205.2	199.6	7.3
Burn characteristics				
Burn 1 time (sec)	193.4	190.9		
Coast arc 1-2 (deg)	144.1	144.0		
Burn 2 time (sec)	69.5	67.9		
Coast arc 2-3 (deg)	98.5	98.5		
Burn 3 time (sec)	26.6	25.8		

orbit (150 X 150 nmi alt). Also, the Aerospace model used a simplified park orbit model, where the other orbital elements were set to zero (Table 1).

There was good agreement with each orbital element in each of the orbits for the Aerospace and NASA GRC models (with the exception of node, which was reference frame and initial state vector dependent) (Table 1). With the agreement between the two 3B transfer models established, the analysis was then ready for re-introduction of the detailed Centaur propulsive characteristics (i.e. hardware drops, propellant boiloffs, settlings, etc.) as well as the adjustments to parking and final orbit state conditions, and the other analysis ground rules.

#### D. Analysis Ground Rules

Two sets of slightly different initial and final orbits were used in this study. In the comparison of the Aerospace Corporation's 3B transfer to that of NASA Glenn's 3B transfer (see preceding section), a Space Shuttle 150 nmi near circular, 28.45° inclined parking orbit to a 300 nmi perigee altitude Molniya orbit transfer was used.<sup>3,4</sup> These data are the first and second columns in Table 1. For the comparison of the Glenn 3B transfer to the standard 2B transfer, inclination variation analyses, launch window analyses, and ground track assessments, a slightly different set of initial and final orbits were used.<sup>5,6,7</sup> The data of these transfers are the third and fourth columns in Table 1. The 3B data was taken from Ref. 3 ("mini-Colt") and 2B data was taken from Ref. 7 ("Colt"). (Note: almost all of the data contained in this paper is archival, originally created by the author, but with no practical way to easily re-run any of the analyses due to obsolete software. Thus, some gaps in the analysis appear in this paper.) Figure 5 illustrates the baseline 3B transfer to Molniya orbit represented by column 3 (mini-Colt data) in Table 1.

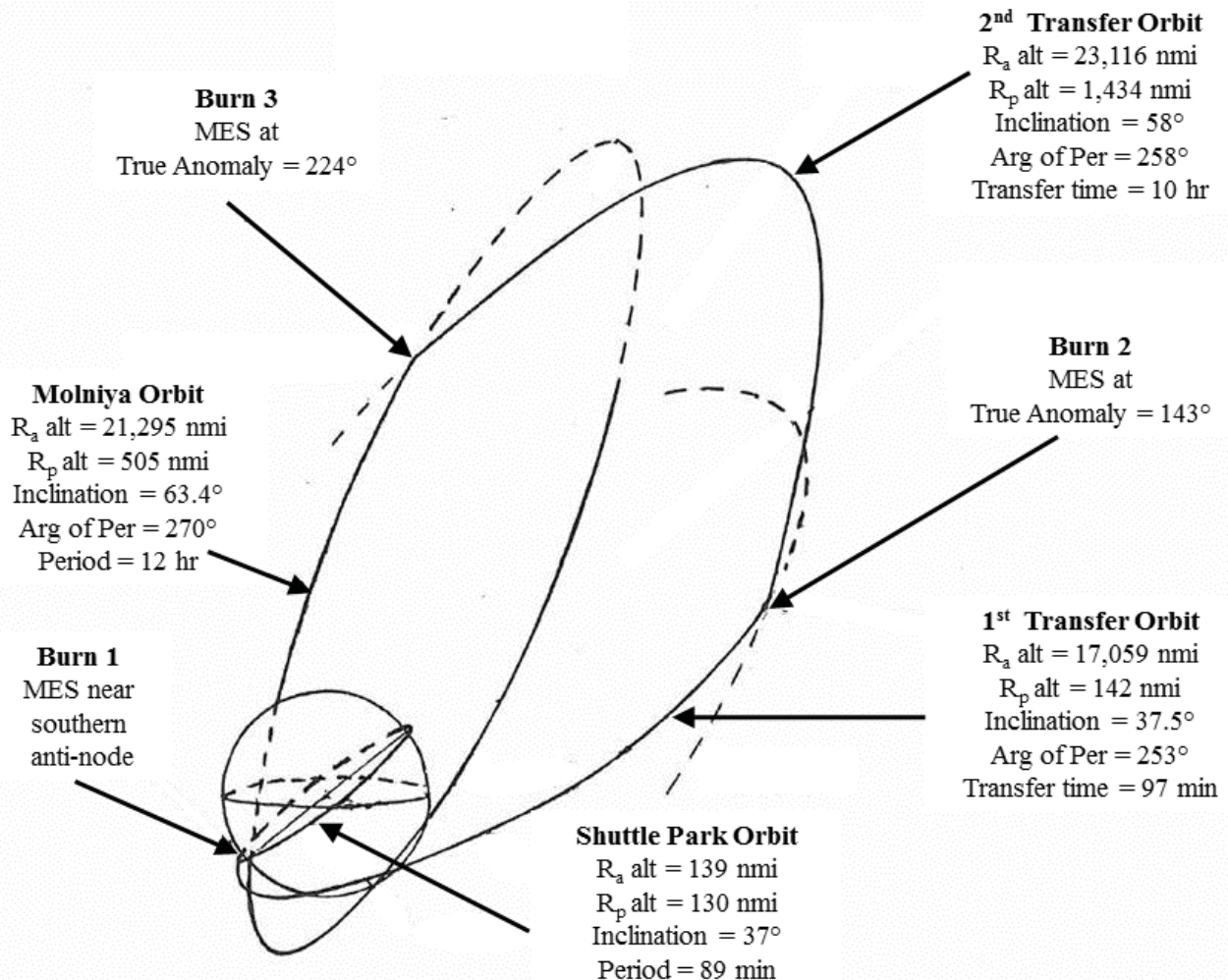


Figure 5. Three Burn Transfer to Molniya Orbit.

All Shuttle/Centaur G modeling data was taken or extrapolated from the Colt and mini-Colt, including electrical power, propellant loadings, residuals, boiloffs, and reaction control system (RCS) usage. Usages associated with the third burn were assumed to be the same as second burn usages (except for the second transfer orbit coast boiloff, which was estimated from the first transfer orbit coast based on time). Appendix A contains 2B and 3B Centaur propellant tanking information. Appendix B contains RL10A-3-3B engine modeling. Appendix C contains net payload calculations. Appendix D contains LH<sub>2</sub> boiloff and RCS usage modeling. Space Shuttle lift commitment varied from 60,500 lbs at LAZ = 90° (i.e. parking orbit  $i = 28.45^\circ$ ) to 43,900 lbs at LAZ=35° (i.e. parking orbit  $i = 57^\circ$ ).<sup>3</sup> Note that Shuttle lift commitment included CISS + Orbiter supplied chargeables = ~9,267 lbs.<sup>3</sup>

While the vehicle and mission were national defense-oriented, all data used and references discussed in this paper are unclassified. Further, no then-proprietary information was used. The Molniya mission parameters are “generic” and were published as such in the open literature and unclassified documents of that time period. There is no mission peculiar information in this work.

### III. Comparing 3B to 2B Transfers

#### A. Overview: How Orbital Elements Changed in 3B vs. 2B

A comparison of how the four orbital elements of interest (semi-major axis ( $a$ ), radius of the perigee ( $R_p$ ), inclination ( $i$ ), argument of the perigee ( $\omega$ )) changed throughout the mission for both the 2B and 3B transfers is shown in Fig. 6. Though generally representative of the change in state conditions shown in Table 1 (columns 3 & 4), the specific values were based on data from the mini-Colt and Colt (Ref. 3 & 7), averaging the values from Main Engine Start (MES) and Main Engine Cut-Off (MECO) of each burn. Though the starting park orbits were similar, they differed significantly in inclination: 37° for 3B vs. 57° for 2B. The reason for using these different parking orbit inclinations was to maximize launch vehicle performance for each transfer. As will be shown and explained in a later section, these maximized separated spacecraft weights at Molniya injection (despite a 20° parking orbit inclination difference) were almost the same. For that reason, the changes in elements on a percentage basis were plotted rather than absolute values in order to compare 3B to 2B. That is, 100% percent represents the total amount of change needed in a particular orbital element for 3B (or 2B) transfer from the park orbit to a Molniya orbit. One complication illustrated in Fig. 6 was that some changes were not additively increasing. That is, some burns increased the values of certain elements beyond their final Molniya values, only to have a later burn reverse direction and reduce these values. These negative changes are represented graphically as overlaid fills in Fig. 6. (For example: the ‘ $a$ ’ change for the 3B transfer shows a narrow vertical bar for Burn 2 overlaid by the narrow horizontal bar of Burn 3, bringing the total bar down to 100%.) Similar reversals occur with Burns 2 & 3 for changes in  $R_p$  for 3B, and also Burns 1 & 2 changes in  $\omega$  for 2B. In addition, two of the stacked bars are significantly greater in percentage magnitude and thus extend beyond the given scale (243% for  $\omega$  in 2B and 358% in  $R_p$  in 3B). Their upper values are merely noted in Fig. 6. The following description is given on the comparisons of the changes, with a detailed explanation of why the optimization changed the elements as it did from a physics and calculus perspective in a later section.

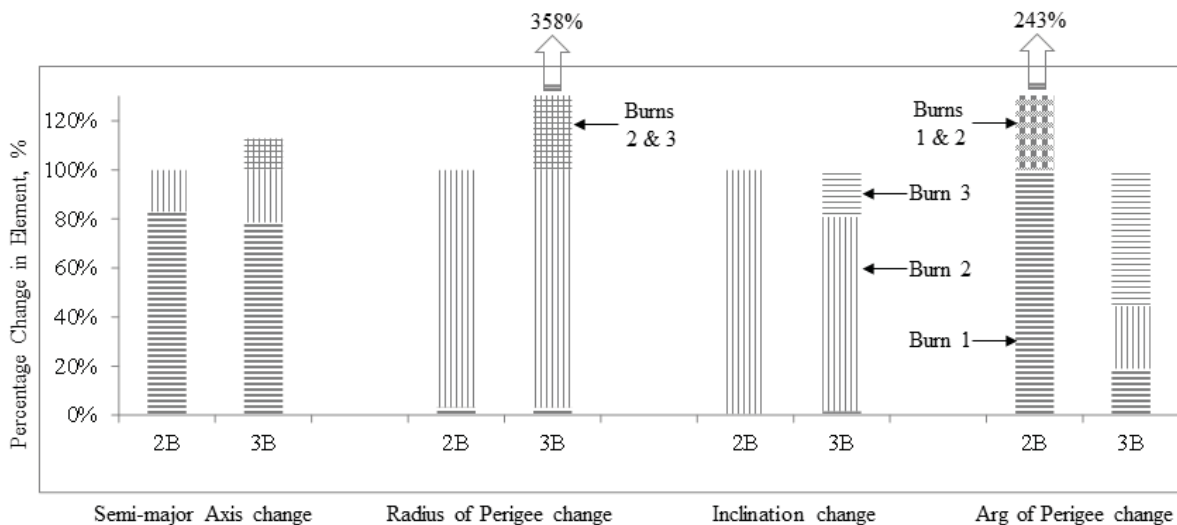


Figure 6. Orbital Element Changes for Two and Three Burn Transfers.



The 'a' was increased predominantly by Burn 1 in both the 2B & 3B transfers (columns 1 & 2 in Fig. 6). While Burn 2 supplied a modest final increase in 2B, it greatly increased 'a' by 3,674 nmi, which was well beyond its 100% value for the 3B transfer. This large overshoot was unusual in trajectory design. Total orbital energy (which goes as the 'a') almost always continually increases throughout a transfer until the final orbit (which is at the greatest total energy) is achieved. Indeed, a transfer orbit of greater orbital energy than the final orbit is almost always a case of 'wasting' performance and presumably non-optimal. As will be explained, a complex interaction existed between the optimized in- and out-of-plane steering, as well as the orbit element trade space, which was responsible for the existence of an optimal solution using a transfer orbit of greater energy than that the final orbit. This is illustrated in Fig. 6 in the 3B bar, where Burn 2 is shown as a narrow vertical filled bar with Burn 3 overlaid as a narrow horizontal filled bar. The retrograde Burn 3 reduced the final value to 100%.

The  $R_p$  was essentially unaffected by Burn 1 in 2B & 3B since the vehicle was at perigee (columns 3 & 4 in Fig. 6).  $R_p$  was raised solely by Burn 2 in the 2B transfer. For the 3B transfer, however, Burn 2 actually extended  $R_p$  well off the scale of Fig. 6 to a value of 358% (i.e. a 1,292 nmi increase in perigee altitude, a value of >3X the vertical scale of Fig. 6). The retrograde Burn 3 then reduced the  $R_p$  by 929 nmi, down to its 100% level. The reason for this overshoot is tied to the preceding discussion pertaining to 'a'.

Figure 6 shows that the inclination change was done entirely by Burn 2 for 2B, while only 80% was done by Burn 2 for 3B (with Burn 3 doing almost all of the remaining change) (columns 5 & 6 in Fig. 6). Burn 1 did negligible inclination change for either 2B & 3B since inclination change is a function of only out of plane thrust component and can be accomplished with less  $\Delta V$  when applied at low orbital velocities (favoring high altitudes).

The  $\omega$  change was considerably different in 2B vs. 3B (columns 7 & 8 in Fig. 6). It is important to first recognize that for a circular orbit,  $\omega$  is undefined, and can change significantly for a near-circular orbit even with minor propulsive thrust. For 2B, Burn 1 changed  $\omega$  well beyond (243%) the Molniya value (i.e. twice the vertical scale shown). Burn 2 then reversed this change and significantly brought  $\omega$  to its final value. Note that Burn 1 is illustrated as thick horizontal fill, while Burn 2 is shown overlaid as thick vertical fill (unlike the other bars which show Burn 2 as thin vertical fill; a consequence of the limitations within the graphical software.) For 3B,  $\omega$  was changed 20% and 25% during Burns 1 & 2 respectively, leaving the majority (55%) of the change for Burn 3.

To gain insight into why the optimization arrived at these solutions (Table 1 and Fig. 6), the Centaur G steering angles, burn times, and time derivatives of the orbital elements (as functions of the steering angles) will be discussed. If all three of the angular components of thrust were known, they could be used with the

**Table 2. Main Burn Steering Characteristics.**

	3 Burn Aerospace PhD Thesis	3 Burn NASA GRC	3 Burn Aug 1984 mini-Colt	2 Burn Oct 1985 Colt
Burn 1 of duration (seconds)	193.4	190.9	284.82	212.3
MES-1 state				
T & N angles (sign)	-3.1150	-3.0148	+ & +	+ & -
W angle (yaw) (deg)	9.2430	-9.1460	-10.3800	-5.2795
W angle rate of change (deg/sec)	-0.0333	0.0330	0.0337	0.0364
MECO-1 state				
T & N angles (sign)			+ & +	+ & -
W angle (yaw) (deg)			-1.537	1.6530
W angle rate of change (deg/sec)			0.0268	0.0302
Burn 2 of duration (seconds)	69.5	67.9	97.6	29.6
MES-2 state				
T & N angles (sign)			+ & +	+ & +
W angle (yaw) (deg)			72.4570	64.8749
W angle rate of change (deg/sec)			-0.0968	-0.1562
MECO-2 state				
T & N angles (sign)			+ & +	+ & +
W angle (yaw) (deg)			55.4149	59.6375
W angle rate of change (deg/sec)			-0.0409	-0.0365
Burn 3 of duration (seconds)	26.6	25.8	27.0	---
MES-3 state				
T & N angles (sign)			- & +	---
W angle (yaw) (deg)			-53.4281	---
W angle rate of change (deg/sec)			-0.2703	---
MECO-3 state				
T & N angles (sign)			- & +	---
W angle (yaw) (deg)			-61.8898	---
W angle rate of change (deg/sec)			-0.0740	---
Thrust / weight (initial)	1.0000	1.0074		
Thrust / weight (final)	2.8045	2.8963		
Total Delta V (ft/sec)	14930.16	14943.40		
Mass (final)/Mass (initial)	0.3566	0.3457		

time derivatives of the orbital elements to calculate the instantaneous change in each element to clarify the results of the optimization. While the archived trajectory output contained pitch and yaw steering angles (and their derivatives), these angles unfortunately were not calculated for the same coordinate system (for reasons lost to time). While the out of plane (yaw) steering data was in the orbital plane system, the pitch angle steering data was with respect to a local horizontal plane system. Thus in-trajectory-plane steering angle and their rates of change could not be used with the time derivative equations (discussed below), though their sign could be inferred. The out-of-trajectory-plane steering data however was available in the output files, so the yaw angle data is given in Table 2 and will be used in this assessment. Since the trajectories cannot be readily re-run, this paper must rely of what is available in the historic output files. The “T-N-W” coordinate system for these derivatives is a rotating reference frame centered at the Centaur/spacecraft within the instantaneous orbital plane. The T vector is tangent to the flight path and in the orbital plane. The N vector is normal to the flight path and also in-plane. The W vector is out of the orbital plane and positive when the acceleration is positive (i.e. in the direction of the angular momentum vector).

The time derivatives of the orbital elements can be expressed as functions of the orbital elements themselves and components of the perturbative acceleration vector (i.e. thrust), in terms of in-plane and out of plane components. Equations 1 through 4 are the time derivatives for semi-major axis, radius of the perigee, inclination, and argument of the perigee respectively.<sup>11</sup> Although the LEOs for the 3B and 2B transfers varied significantly in inclination (37° vs. 57° respectively), meaningful comparisons between the two transfers can still be made by examining the solutions of Equations 1- 4 and the corresponding steering angles (Table 2). Using the orbital element values from the trajectories based on data in the mini-Colt and Colt (consistent with the orbital data in Table 1), the coefficients for each thrust vector component were calculated for 3B and 2B using Equations 1- 4, averaging the MES and MECO values. The results of these calculations appear in Table 3.

$$\frac{\partial a}{\partial t} = \left[ \frac{2a^2 V}{\mu} \right] T \quad (1)$$

$$\frac{\partial R_p}{\partial t} = \frac{1}{V} \left\{ \left[ 2R_p \frac{1 - \cos \theta}{1 + e} \right] T + [r \sin \theta] N \right\} \quad (2)$$

$$\frac{\partial i}{\partial t} = \left[ \frac{r}{\sqrt{l\mu}} \cos(\theta + \omega) \right] W \quad (3)$$

$$\frac{\partial \omega}{\partial t} = \frac{1}{V} \left\{ \left[ \frac{2 \sin \theta}{e} \right] T + \frac{r}{le} (2e + \cos \theta + e^2 \cos \theta) N - \left[ \frac{rV}{\sqrt{l\mu}} \sin(\theta + \omega) \cot i \right] W \right\} \quad (4)$$

The values in Table 3 can be viewed as indicators of the relative ease of changing the orbital elements at particular points in orbits. As will be shown, the total vehicle performance of the 3B transfer was almost identical to that of the 2B transfer. Thus, the coefficients in Table 3 in the aggregate represent approximate equivalent difficulty paths leading to a comparable result (i.e. comparable mass to Molniya orbit). The combination of the Table 3 coefficients, the thrust component for each element, and the burn time can provide insight to the variationally-derived values in Fig. 6. For example: the variationally-derived change in semi-major axis for Burn 1 in 3B transfer was 8,466 nmi. The rough approximation would be the combination of the Table 3 value (4,485 sec), the thrust component (0.00345 nmi/sec<sup>2</sup>), and the burn time (285 sec), yielding 4,410 nmi. Thus, while this linear approximation of a non-linear burn is in error by a factor of two, it is still adequate to discuss general trends.

## B. The 3B Transfer

The first burn (“Burn 1”) was 285 seconds long and was 70% of the sum of the three orbital burn times. Burn 1 was essentially planar and occurred well into the third quadrant of the argument of the latitude ( $u$ ); that is, just before the southern antinode. It primarily increased the orbital energy (thus ‘a’, thus the period). It also generally fixed the perigee, and likewise the  $\omega$  of the final orbit. Burn 1 was largely within the orbital plane and raised apogee altitude to ~17,059 nmi (~80% of Molniya apogee altitude of 21,295 nmi). The burn also rotated the  $\omega$  to 253°, only 17° short of Molniya’s 270°. (Note:  $\omega$  value does not correspond to park orbit in Table 1 due to rapidly changing

near-zero eccentricity early in the finite burn.) The  $i$  and  $R_p$  were almost totally unchanged from that of the parking orbit. The first transfer orbit extended from  $10.5^\circ$  to  $143.4^\circ$  of true anomaly ( $\theta$ ) and was 1.6 hours in duration.

The Burn 1 coefficients of the perturbations (Equations 1-4) appear in Table 3. The coefficient for the semi-major axis ( $a$ ) derivative (Equation 1) was positive (4,485 sec), and since the optimization showed a large increase in ‘ $a$ ’, then the in-plane thrust component T must be large and positive. The coefficients in the  $R_p$  derivative were de minimis (Equation 2) since Burn 1 took place at perigee. The combination of the small negative coefficient for the inclination ( $i$ ) derivative of -0.0595sec/nmi (Equation 3) and

the small negative ( $-10.4^\circ$  at MES and  $-1.5^\circ$  at MECO) out of plane thrust component W (Table 2) illustrated why almost no plane change was performed in Burn 1. Since W was negative and the out of plane coefficient for  $\omega$  was positive (0.2594 sec/nmi), its product was negative. Since  $\omega$  increased, then the in-plane thrust component N must also be positive in order for its combination with its larger coefficient (0.8351 sec/nmi) to be greater than that of the out on plane combination. (The coefficient of T was smaller (0.0544 sec/nmi) than that of N, yielding a combination likely to be smaller.) Note that the in-plane coefficients were all positive, while the out of plane coefficients ( $i$  and  $\omega$ ) were of differing sign. Thus, out-of-plane thrust driven changes in  $i$  and  $\omega$  would be at cross purposes.

The second burn (Burn 2) was 98 seconds in duration. It occurred in the first quadrant of ‘ $u$ ’; that is, just after the node. Burn 2 was significantly both in- and out-of-plane, raising  $R_p$  considerably and further increasing ‘ $a$ ’, while at the same time increasing ‘ $i$ ’. ‘ $a$ ’ was increased by 3,674 nmi to a value of 15,713nmi (which was 1,375 nmi greater than Molniya). This corresponded to a perigee increased to 1,434 nmi altitude (alt) from the first transfer orbit ( $\sim 142$  nmi alt), and an apogee increased to 23,116 nmi alt (1,821 nmi higher than Molniya orbit apogee of 21,295 nmi alt). This is one of the most remarkable aspects of the 3B solution, since orbit-to-orbit transfers almost always increase in total energy (which is directly proportional to semi-major axis) until the final orbit is reached. The inclination was greatly increased from the first transfer orbit of  $37.5^\circ$  to the second transfer orbit of  $58.3^\circ$ . The  $\omega$  was increased  $5.5^\circ$  to a value of  $258.2^\circ$ . The second transfer orbit extended from  $127^\circ$  to  $224^\circ$  of  $\theta$  and was 10.1 hours in duration.

The Burn 2 coefficients of the perturbations were quite different than those of Burn 1. The coefficient for the ‘ $a$ ’ derivative (Equation 1) was large and positive (11,004 sec; Table 3), and since the optimization showed an increasing ‘ $a$ ’, then the in-plane thrust component T must be positive. The  $R_p$  coefficients were also both large and positive (4,796 and 5,564 sec for T & N respectively; Table 3), and since  $R_p$  had to be raised, both in-plane thrust components T & N were positive. The combination of the large positive coefficient for the inclination derivative of 0.5707 sec/nmi (Table 3) and the large positive ( $72.5^\circ$  at MES and  $55.4^\circ$  at MECO; Table 2) out of plane steering component illustrate why the large plane change of  $21^\circ$  was possible. The  $\omega$  increase was due to the sum of the combinations of the large, positive in-plane perturbation coefficients (1.1331 and 0.5318 sec/nmi) (Equation 4) and in-plane thrust components being greater than the out of plane combination with the coefficient -0.3068 sec/nmi. Similar to Burn 1, in Burn 2, the in-plane coefficients were all positive, while the out of plane coefficients ( $i$  and  $\omega$ ) were of differing sign. Thus, out-of-plane thrust driven changes in  $i$  and  $\omega$  would be at cross purposes.

The third burn (Burn 3) was the shortest at 27 seconds duration. It occurred in the second quadrant of ‘ $u$ ’; that is, approaching the descending node. (An oddity of the solution is that Burn 3 was located in the general vicinity of the alternate second burn location for a 2B transfer.) Like Burn 2, Burn 3 was also significantly both in- and out-of-plane. However, Burn 3 was retrograde. It performed the majority of the  $\omega$  change ( $\sim 12^\circ$ ) while also reducing ‘ $a$ ’

**Table 3. Coefficients of Estimated Time Derivatives of Orbital Elements.**

		3 Burn			2 Burn		
		T	N	W	T	N	W
Burn 1							
	$\Delta a/\Delta t$ :	4,485	---	---	4,629	---	---
	$\Delta R_p/\Delta t$ :	1	34	---	2	-40	---
	$\Delta i/\Delta t$ :	---	---	-0.0595	---	---	-0.0129
	$\Delta \omega/\Delta t$ :	0.0544	0.8351	0.2594	-0.0630	0.8112	0.1331
Burn 2							
	$\Delta a/\Delta t$ :	11,004	---	---	13,183	---	---
	$\Delta R_p/\Delta t$ :	4,796	5,564	---	3,095	4,011	---
	$\Delta i/\Delta t$ :	---	---	0.5707	---	---	0.4649
	$\Delta \omega/\Delta t$ :	1.1331	0.5318	-0.3068	0.9600	0.5525	-0.1932
Burn 3							
	$\Delta a/\Delta t$ :	11,882	---	---	---	---	---
	$\Delta R_p/\Delta t$ :	5,491	-6,402	---	---	---	---
	$\Delta i/\Delta t$ :	---	---	-0.4276	---	---	---
	$\Delta \omega/\Delta t$ :	-1.1184	0.5142	-0.3389	---	---	---

(by 1,375 nmi) and  $R_p$  (by 929 nmi) to their Molniya values. A modest amount of plane change was also performed ( $5^\circ$ ). True anomaly at injection was  $217.0^\circ$ .

Burn 3 coefficients of the perturbations (Table 3) were quite different than those of Burns 1 or 2, both in sign and magnitude. The coefficient of 'a' derivative (Equation 1) was very large and positive (11,882 sec), and since the optimization showed a decreasing 'a', then the in-plane thrust component T had to be negative. The  $R_p$  coefficients were also both large (5,491 and -6,402 sec for T & N respectively; Equation 2), and since  $R_p$  had to be lowered, in-plane thrust component N was most likely positive, while T is indeterminate (though likely negative). The combination of the moderate coefficient for the inclination derivative (Equation 3) of  $-0.4276$  sec/nmi and the large negative ( $-53.4^\circ$  at MES and  $-61.9^\circ$  at MECO) out of plane steering component for Burn 3 (Table 2) enabled the modest positive plane change. The considerable negative out of plane component W together with the  $\omega$  coefficient in Table 3 of  $-0.3389$  sec/nmi (Equation 4) yielded a positive value, which was also true of the (likely) negative value of the in-plane component T taken with its coefficient  $-1.1184$  sec/nmi. The positive in-plane component N with its Table 3  $\omega$  coefficient  $0.5142$  sec/nmi also yielded a positive value. Unlike Burn 2, in Burn 3, the in-plane coefficients were of varying sign, while the out of plane coefficients (i and  $\omega$ ) were both negative. Thus, the negative out-of-plane thrust driven changes in i and  $\omega$  had the effect of increasing both inclination and  $\omega$ .

### C. The 2B Transfer

Burn 1 was 212 seconds long and was 88% of the sum of the two orbital burn times. Like the 3B transfer, Burn 1 was essentially planar and occurred well into the third quadrant of the argument of the latitude (u); that is, just before the southern antinode. It primarily increased the orbital energy (thus 'a', thus the period). It also generally fixed the perigee, and likewise the  $\omega$  of the final orbit. Burn 1 was largely within the orbital plane and raised apogee altitude to 17,954 nmi (~84% of Molniya apogee altitude of 21,295 nmi). The burn also reduced the  $\omega$  to  $266^\circ$ , slightly overshooting the Molniya value, leaving it  $4^\circ$  short of Molniya's  $270^\circ$ . (Note:  $\omega$  value does not correspond to park orbit in Table 1 due to rapidly changing near-zero eccentricity early in the finite burn.) The i and  $R_p$  were almost totally unchanged from the parking orbit. The transfer orbit extended from  $8.2^\circ$  to  $130.8^\circ$  of true anomaly ( $\theta$ ) and was 68 minutes in duration.

Burn 1 coefficients of the perturbations (Equations 1- 4) for the 2B transfer also appear in Table 3 and were very similar (both in magnitude and sign) to those of the 3B transfer. The coefficient for the 'a' derivative (Equation 1) was positive (4,629 sec), and since the optimization showed an increasing 'a', then the in-plane thrust component T must be large and positive. Similar to the 3B case, the coefficients in the  $R_p$  derivative (Equation 2) were de minimis since Burn 1 took place at perigee. The combination of the small negative coefficient for the 'i' derivative (Equation 3) of  $-0.0129$ sec/nmi and the small, mostly negative ( $-5.3^\circ$  at MES and  $1.6^\circ$  at MECO) out of plane thrust component W (Table 2) illustrated why almost no plane change was performed in Burn 1 for the 2B transfer. Since W was mostly negative and the out of plane coefficient was positive, its combination was negative. Since  $\omega$  decreased, overshooting its final Molniya value, then in-plane thrust components T & N were most likely positive (where  $T > N$ ) in order for the sum of the combinations to be less than that of the out-of-plane combination. (The coefficient of T was likely larger than N since the burn was primarily an orbit raising maneuver. Further, the T coefficient ( $-0.0630$  sec/nmi) was smaller than the N coefficient ( $0.8112$  sec/nmi).) Note that the in-plane coefficients were not all positive, though small angle averages were the real reason for this occurrence. The out of plane coefficients (i and  $\omega$ ), like in the case of 3B, were of opposite sign, thus, changes in i and  $\omega$  would be at cross purposes. This set up a major difference between 2B and 3B. Since the i and  $\omega$  coefficients were of opposite sign in both Burn 1 & 2, and inclination had to be changed in Burn 2, this forced most of the  $\omega$  change into Burn 1. Indeed, the  $\omega$  change had to overshoot the target value of  $270^\circ$  in order to enable the positive change for inclination.

Burn 2 was 30 seconds in duration. It occurred in the first quadrant of 'u'; that is, just after the node. Burn 2 was significantly both in- and out-of-plane, raising all elements to their Molniya values. 'a' was increased by 1,849 nmi to a Molniya value of 14,335 nmi. The  $R_p$  was increased 360 nmi to a Molniya orbit perigee of 502 nmi alt. The inclination was increased  $6.4^\circ$  to a final Molniya value of  $63.4^\circ$ . The  $\omega$  was increased  $3.8^\circ$  to a Molniya value of  $270^\circ$ . True anomaly at injection was  $124.9^\circ$ .

Burn 2 coefficients of the perturbations (Table 2) for 2B transfer were similar to those of the 3B transfer in terms of sign and magnitude. The coefficient for the semi-major axis (a) derivative (Equation 1) was very large and positive (13,183 sec), and since the optimization showed an increasing 'a', then the in-plane thrust component T must be positive. The  $R_p$  coefficients were also both large and positive (3,095 and 4,011 sec for T & N respectively; Equation 2), and since  $R_p$  had to be raised, both in-plane thrust components T & N were positive. The combination of the positive coefficient for the inclination derivative (Equation 3) of  $0.4649$  sec/nmi and the positive ( $64.9^\circ$  at MES and  $59.6^\circ$  at MECO) out of plane steering component illustrate why the entire plane change was performed by Burn 2. The considerable positive out-of-plane steering component W together with its coefficient of  $-0.1932$

sec/nmi (Equation 4) yielded a negative value, which suggested that one or both of the in-plane components T & N were sufficiently positive to produce a sum of their combinations (with their coefficients 0.9600 and 0.5525sec/nmi respectively) that was greater than that of the out-of-plane combination.

#### D. Summary Observations: 3B vs. 2B

Several observations can be made pertaining to the existence of an optimal three burn transfer which yielded almost identical performance as a two burn transfer, despite the considerable additional inclination change performed (20°). Comparing 3B to 2B orbital element derivative coefficients for each burn provided insight as to why it was desirable to increase both the 'a' and  $R_p$  well beyond their final requirements, only to reduce them back down after changes were made in both  $i$  and  $\omega$ .

The magnitudes of each of the derivative coefficients in Burn 1 for both 3B and 2B were comparable, as were their signs (with some exceptions for those of small absolute values). The 3B and 2B coefficients for 'a' were almost the same and produced similar results. This was consistent with the expectation that Burn 1 was primarily an apogee raising maneuver ( $R_p$  change was approximately zero since the Burn 1 was at perigee, reflected by de minimus coefficients). The coefficients for inclination were also small and comparable for both 3B and 2B, producing almost no plane change since it was not optimal to do so at high speed (i.e. at perigee). The 3B and 2B coefficients for  $\omega$  were roughly comparable in magnitude, but with a difference in sign for T. Although the percentage change in  $\omega$  was large in 2B (Fig. 6), the actual value (like all  $\omega$  changes) was small (~ 6½°). The range in thrust components was similar in magnitude and sign. Although the burn time for 3B was ½ greater than that for 2B (285 vs. 212 seconds respectively), with somewhat similar thrust angles, it did not produce greater changes in the orbital elements compared to the 2B transfer. Thus with the exception of the large percentage changes in  $\omega$ , the changes in the other orbital elements done by Burn 1 in 3B and 2B were similar (as illustrated in Fig. 6).

Unlike Burn 1, the magnitudes of each of the Burn 2 derivative coefficients for 3B and 2B were noticeably different. The 2B 'a' value was surprisingly greater than the 3B value, despite the fact that the 3B increase in 'a' was proportionately larger than 2B's. This greater increase in 'a' was due largely by the 3B Burn 2 time which was triple that of 2B's Burn 2 (~98 vs. ~30 seconds). Nevertheless, the change in 'a' in 2B was facilitated by its larger coefficient (13,183 sec vs. 11,004 sec). Also note that the coefficients for 'a' for both 3B and 2B were nearly triple their Burn 1 values. The 2B coefficients for  $R_p$  were ~ ½ of the value of the 3B coefficients. Combined with the triple burn time, the 3B  $R_p$  coefficients illustrated the greater ease in  $R_p$  increase (Fig. 6). The inclination coefficient was greater for 3B (keeping in mind that the units are radians/sec). It was this greater inclination coefficient and splitting up the plane change between Burns 2 & 3 in the 3B solution, which led in large part to the existence of a three burn solution to Molniya orbit. Though all of the plane change in 2B was done in Burn 2, while only 80% was done in 3B, the absolute values of these changes were 6.4° vs. 21° respectively. (Later, it will be shown that requiring a large change in inclination (i.e. a lower inclination parking orbit) was fundamental to the very existence of a three burn transfer.) While the  $\omega$  coefficients were slightly more favorable for the 3B transfer, the 2B percentage change in  $\omega$  was large, though the absolute value of the  $\omega$  change in 3B was greater. The thrust components' magnitudes and signs were comparable for 2B and 3B.

Burn 3 was largely to complete the inclination and  $\omega$  change, while subtracting out the excess 'a' and  $R_p$  altitude. The 'a' coefficient was greater (i.e. more favorable) for Burn 3 than it was in Burn 2. The same was also true of the  $R_p$  coefficients, which were also greater than their absolute values in Burn 2. The inclination coefficient was smaller than that in Burn 2, but still significant to enable the remaining 5° plane change. The  $\omega$  coefficients were comparable to those in Burn 2, enabling the remaining significant change in  $\omega$  to its final value. It was also interesting to compare 3B's Burn 3 coefficients to those of 2B's Burn 2. While the 'a' coefficients were almost comparable, the  $R_p$  coefficients for 3B were significantly greater. 3B's inclination coefficient was slightly lower than that of 2B, while 3B's  $\omega$  coefficients were greater. All of this suggests that the orbital element space of 3B's Burn 3 was generally more attractive than those of 2B's Burn 2.

But it was the  $\omega$  coefficients which implied why it was advantageous to incur these two losses: because the thrust component T was negative while its coefficient is large and negative (yielding a positive combination). Similarly, both the N & W components yielded positive combinations. Thus the entire  $\omega$  derivative yielded a significant positive sum (unlike in Burn 2). Further, compared to 2B's Burn 2 case, even though the burn times were almost the same, the coefficients did not complement, but competed, producing a much smaller change in  $\omega$  in absolute terms.

Why an optimal 3B solution existed despite greater propellant usage and an intermediate transfer orbit with greater energy than the final orbit was apparent by observing that:

- Orbital element derivative coefficients for 3B's Burns 2 & 3 were mostly greater than 2B's Burn 2
- Orbital element change-spaces for 3B were more delta V-efficient in the aggregate
- Splitting up changes into Burns 2 & 3 enabled more optimal changes

- Yaw derivative coefficients were of opposite sign for  $i$  &  $\omega$  in 2B, forcing costly  $\omega$  changes into Burn 1 (where instead, 3B could defer them into Burn 3)
- Derivative for  $\omega$  was a function of both in- and out-of plane thrust components (coupling effects)
- (As will be shown in next section) significant change in 'i' was necessary for existence of 3B solution
- Derivative coefficients in 3B's Burn 3 in-plane elements were opposite in sign, enabling retrograde burns be done to subtract out excess  $a$  &  $R_p$ , while still enabling large changes in  $i$  &  $\omega$

In summary: the 3B transfer with comparable performance existed because it was more advantageous to split up and perform the 'i' and  $\omega$  changes in more favorable orbital element spaces even though it cost performance to temporarily increase 'a' and  $R_p$  beyond their required Molniya values (and eventually subtract them back out).

#### IV. Variation with Parking Orbit Inclination

##### A. 3 Burn Transfer as a Function of Parking Orbit Inclination

An analysis was performed on how the 3B transfer changed as parking orbit inclination was varied. As was discussed earlier, the inclination was increased primarily by Burn 2 for 3B transfers. As the park orbit inclination was increased from  $28.45^\circ$  and total plane change required decreased, most of the reduced plane change continued to take place in Burn 2. Fig. 7 illustrates the change in Transfer Orbit 2's inclination. The regions labeled represent the amount of plane change done by Burns 2 & 3. The amount performed by Burn 3 also decreased but at a much smaller rate. Eventually a point was reached where the amount of plane change was small enough that it could be done entirely by Burn 2, with minimal adverse effect on argument of the perigee. At an inclination of  $57^\circ$ , Burn 3 went to zero, the 3B solution vanished and the 3B transfer degenerated into the 2B solution. It is of academic interest to note that Burn 2 could be made to vanish instead, whereby Burn 3 would become the second burn at  $57^\circ$ . This alternate 2B transfer, however, would not be desirable in lieu of the standard 2B transfer due to its longer transfer time. Beyond  $57^\circ$ , only the 2B solution exists. As the parking orbit inclination continued to increase, approaching the Molniya value ( $63.4^\circ$ ), the 2B trajectory reduced to a planar Holman transfer.

The data pertaining to the change in  $R_p$  altitude as a function of park orbit inclination was not archived in the original analysis. However, the change in radius of apogee ( $R_a$ ) altitude for 3B transfer was tabulated and was plotted in Fig. 8.  $R_a$  was seen to significantly decrease with increasing park orbit inclination and had a minimum at  $54^\circ$  inclination. At a park orbit inclination of  $57^\circ$  and above (where the 3B solution vanished)  $R_a$  altitude became that of Molniya's (21,295 nmi).

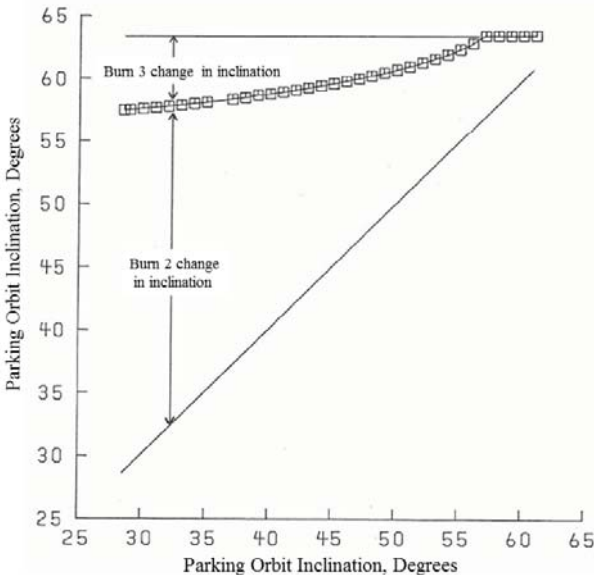


Figure 7. Plane Change vs. Park Orbit Inclination for 3B Transfer.

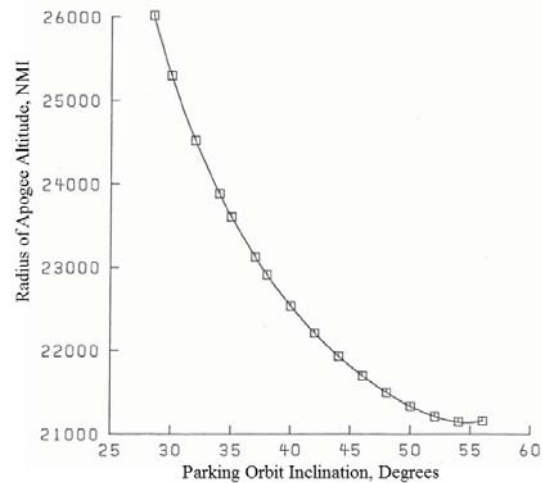
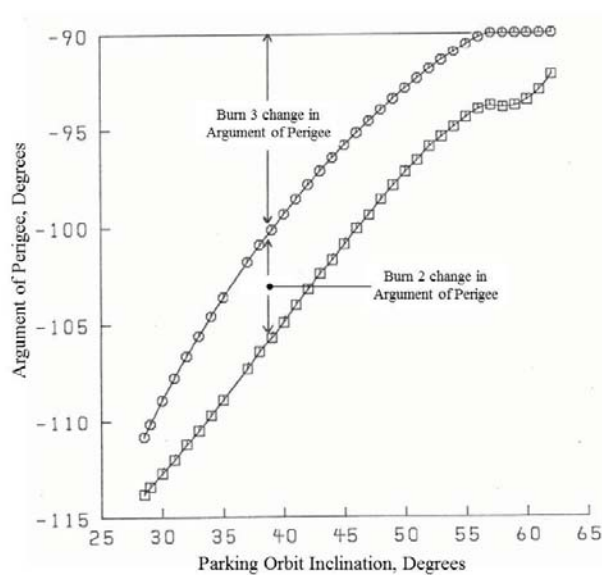
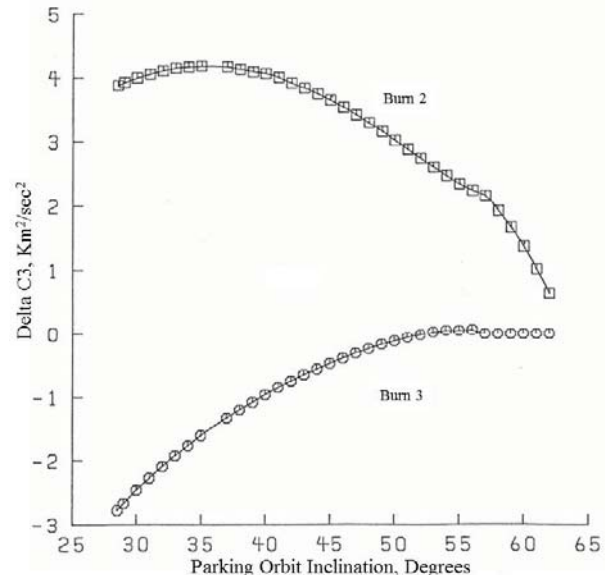


Figure 8. Apogee Radius Change vs. Park Orbit Inclination for 3B Transfer

As was discussed earlier, the majority of the  $\omega$  change was done by Burn 3 for the 3B transfer. As the park orbit inclination was increased from  $28.45^\circ$ , the total  $\omega$  change required decreased. Most of the reduction in  $\omega$  change came from Burn 3, with the amount performed in Burn 2 remarkably constant. Figure 9 showed the change in Transfer Orbit 1 & 2's argument of the perigee. The regions labeled therefore represent the amount of  $\omega$  change



**Figure 9. Argument of Perigee vs. Park Orbit Inclination.**



**Figure 10. Change in C3 vs. Park Orbit Inclination.**

done by Burns 2 & 3. At a park orbit inclination of  $57^\circ$  and above (where the 3B solution vanished) the remaining  $\omega$  change was performed solely by Burn 2. The Burn 1 values for  $\omega$  were not retained from the original analysis.

The change in semi-major axis as a function of park orbit inclination was not archived in the original analysis. However, the change in C3 (orbital energy per unit mass (an analogous quantity)) was tabulated and plotted in Fig. 10. Burn 2 was seen to increase  $\Delta C3$  until a maximum was reached at an inclination of  $36^\circ$ . It then steadily decreased until a parking orbit of  $57^\circ$ , where the  $\Delta C3$  went to zero for Burn 3, greatly reducing the need for large increases in C3 by Burn 2 (thus the change in slope by Burn 2). Burn 3 was always retrograde (i.e. decreased C3) throughout the 3B range of inclinations. As will be discussed in the next section, the maximum which occurred in Burn 2 corresponded to the point where Centaur propellants had to be off-loaded in order to satisfy decreasing Shuttle lift capability (as LAZ decreased to increase park orbit inclination). Thus the  $\Delta C3$  of Transfer Orbit 2 had to decrease above a park orbit inclination of  $36^\circ$ .

### B. Performance vs. Park Orbit Inclination for 3B vs. 2B

An analysis was performed of the variation of certain orbital characteristics for 3B and 2B transfers as a function of parking orbit inclination. This was done to determine total vehicle performance (including identifying the optimum park orbit inclination), understand the orbital mechanics, and begin to determine if there were any mission-driven impacts on vehicle systems. 34 trajectories were run for parking orbit inclinations between  $28.5^\circ$  and  $62^\circ$ .

In order to calculate net separated spacecraft mass (payload) as a function of inclination for both 3B and 2B, two quantities had to be calculated: the “wet Centaur” mass (which included propellant margins and residuals) for 3B and 2B (both fully loaded and off-loaded) and the Shuttle lift capability --- both as a function of park orbit inclination. The wet Centaur tabulation appears in Appendix C. The Shuttle lift capability and its impact on Centaur propellant off-loading and propulsion operation were calculated as follows:

The “Space Shuttle lift commitment” varied from 60,500 lbs at LAZ =  $90^\circ$  (i.e. parking orbit  $i = 28.45^\circ$ ) to 43,900 lbs at LAZ =  $35^\circ$  (i.e. parking orbit  $i = 57^\circ$ ).<sup>3</sup> (Note that Shuttle lift commitment included CISS + Orbiter supplied chargeables =  $\sim 9,267$  lbs).<sup>3</sup> These values were consistent (and slightly conservative) with the “Space Shuttle lift capability” analysis which illustrated that at park orbit inclination of  $57^\circ$ , the Shuttle capability was 45,400 lbs.<sup>12</sup> For every  $1^\circ$  increase in park orbit inclination, the Shuttle lift commitment decreased by 581 lb. At the lower inclinations where the Centaur was fully tanked, every  $1^\circ$  increase meant an increase in total stack performance of approximately 285 lb. From  $28.45^\circ$  to approximately  $35.75^\circ$ , the oxidizer-to-fuel ratio (‘o/f’) equaled 6.1579 and was held constant. This was done for simulation purposes only and did not reflect how the propellant utilization system would actually operate. At  $35.75^\circ$ , the Shuttle lift commitment equaled the combined weight of a fully loaded Centaur and a maximized payload. Beyond that point,  $LO_2$  would be offloaded until the o/f

ratio reached 6.0. This region ( $\sim 1^\circ$  wide) was not simulated. Starting at  $36.75^\circ$  and continuing up to  $62.0^\circ$ , both  $\text{LO}_2$  and  $\text{LH}_2$  were offloaded to maintain a 6:1 mixture ratio. The 2B fuel loading was modeled in a similar manner. All other modeling was unchanged from the baseline. Appendixes A & B contain the detailed explanation of propellant loading and the concomitant engine modeling.

For the fully loaded region, the same “wet Centaur” weight (i.e. Centaur including residuals and propellant margins) was subtracted from the 3B and 2B burnout weights. Likewise, a wet Centaur weight characteristic of an offloaded mission was used for the higher inclination transfers. By plotting maximum payload (i.e. jettison weight – wet Centaur), a one to one comparison could be made between 3B and 2B for a particular inclination. In addition, it allowed the different residuals and reserves associated with full tanked and offload missions to be taken into account. Appendix C contains net payload calculations. Appendix D describes  $\text{LH}_2$  boiloff and RCS usage.

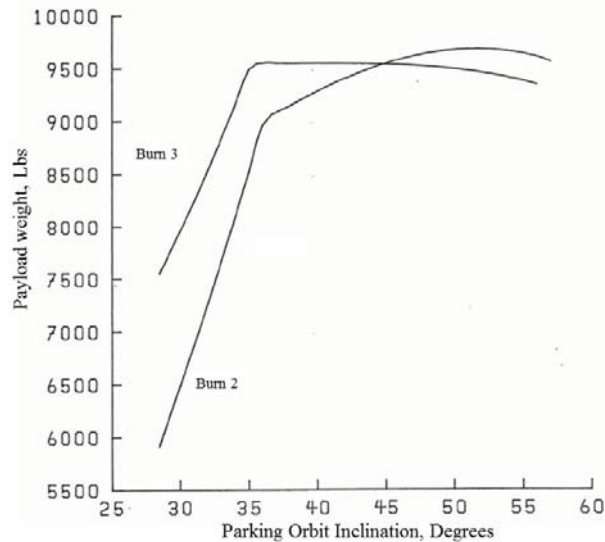


**Figure 11. Performance vs. Park Orbit Inclination for 3B and 2B Transfers**

Figure 11 summarizes the results of 3B vs. 2B performance vs. parking orbit inclination. Performance rapidly increased with inclination as excess Shuttle lift capability was traded for more Shuttle supplied plane change. The knees of the curves correspond to where the Shuttle lift capability (as a function of park orbit inclination) equaled the fully tanked Centaur + payload weight. Centaur offloading started at the knee of each curve ( $\sim 37^\circ$  for 3B,  $\sim 38^\circ$  for 2B). As the park orbit inclination increased further, total system performance leveled off for 3B, then slowly decreased. For 2B however, performance continued to gradually increase, reaching a maximum of 9,682 lb at  $51^\circ$ . (While that was 130 lbs greater than the 2B baseline at  $i = 57^\circ$ , it was decided earlier in the program not to go through the process of establishing a new Shuttle ascent profile. This decision preceded (and was independent of) the 3B to Molniya assessment.) Nevertheless, 3B had better performance than 2B up to a park orbit inclination of  $44^\circ$ . The  $37^\circ$  case represents the peak performance for 3B. Its payload of 9,545 lb was only

7 lb less than the  $57^\circ$  case for 2B (which was the baseline ascent for the 2B transfer). If launched into a  $37^\circ$  parking orbit, 3B performance would be comparable to 2B, but would be fully tanked. This was a major finding of the analysis and satisfied a primary goal of the study.

The performance curves did not coincide at  $57^\circ$  because of the losses associated with the settling phases. As the steady state main impulse went to zero, the fixed settlings, pre-chills, and RCS usages represented reductions in burnout weight that produced little  $\Delta V$  in return. The effects of these losses associated with Burns 2 & 3 could also be estimated by approximating them as drop masses in the integrated trajectory optimization (see Appendix E). For Burn 3 in 3B ( $i = 37^\circ$ ), each pound of propellant for settling took the place of 0.9 lb of payload. The rocket was in effect carrying dead weight through all of the burns, only to throw it away just before it reached the final orbit. These non-main impulse propellants amounted to well over 200 lb of lost performance. As Burn 3 went to zero (at  $i = 57^\circ$ ), the two partials representing the Burn 2 & 3 transients became  $-0.9$  and  $-1.0$  in the limit respectively. It was because 3B had this additional set of settling losses that its performance decreased singularly following the start of offloading, despite the smaller plane changes. The 2B performance continued to benefit from the shrinking plane changes until its second burn became short enough. Then it too began to suffer the same way as 3B.

The variation in duration of Burns 1, 2, and 3 for the 3B transfer are given in Fig. 12. Burn 1 was the longest throughout the range of park orbit inclinations and varied between 282 to 217 seconds. It was followed by Burn 2 which ranged between 101 and 32 seconds. Burn 3 was 35 seconds long at  $28.45^\circ$  and then vanished at  $57^\circ$ . Note that while Burn 1 had a slight maximum at  $35^\circ$  corresponding to the aforementioned onset of Centaur off-loading, Burn 2's slight maximum ( $\sim 1$  second) took place at  $32^\circ$  (explanation unknown). The variation of Burns 1 and 2 for the 2B transfer are given in Fig. 13. Again, Burn 1 was the longest throughout the range of park orbit inclinations and varied between 260 to 214 seconds. Burn 2 steadily decreased, ranging between 194 and 30 seconds; a much greater variation than in the case of 3B. Note that Burn 1 similarly had a modest maximum at  $37^\circ$  corresponding to



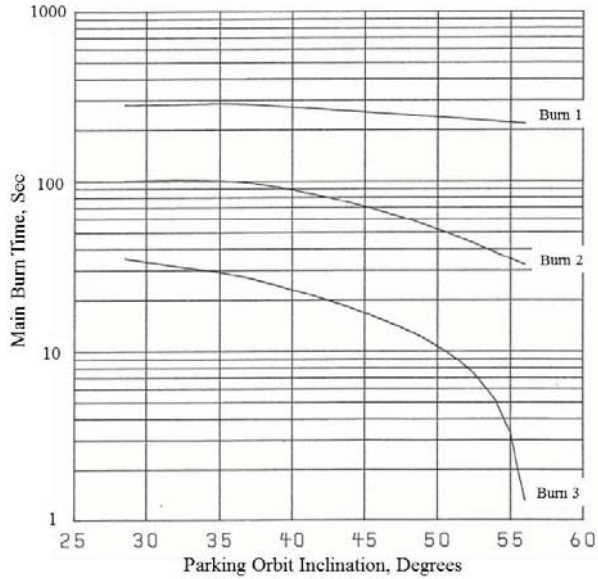


**Figure 12. Main Burn Times vs. Park Orbit Inclination for 3B Transfer.**

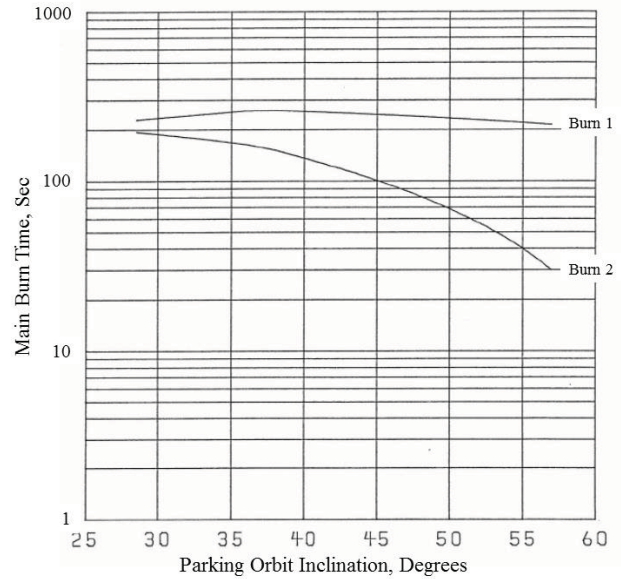


**Figure 13. Main Burn Times vs. Park Orbit Inclination for 2B Transfer.**

the aforementioned start of Centaur off-loading. Note that the 57° case in 2B also represented the asymptotic 3B transfer at that same inclination.

The total “mission elapse times” (MET), which spanned from MES-1 to MECO-3 for 3B, as a function of park orbit inclination were plotted in Fig. 14. The total times ranged from over 14 hours at 28.45° to 10 ½ hrs at 56°. The overall shape of the curve and the minimum at 54° inclination are coincident with the change in  $R_a$  altitude for Burn 2 (Fig. 8). The total MET for 2B (MES-1 to MECO-2) as a function of park orbit inclination were plotted in Fig. 15. The times increased almost linearly from over 64 minutes at 28.45° to 77 minutes at 57°. This order of magnitude increase in MET for 3B vs. 2B represented a major disadvantage for 3B, as more consumables would be needed to perform 3B transfers compared to 2B. The following discussion explains how the need for more consumables could be mitigated with modest changes to the Centaur vehicle.

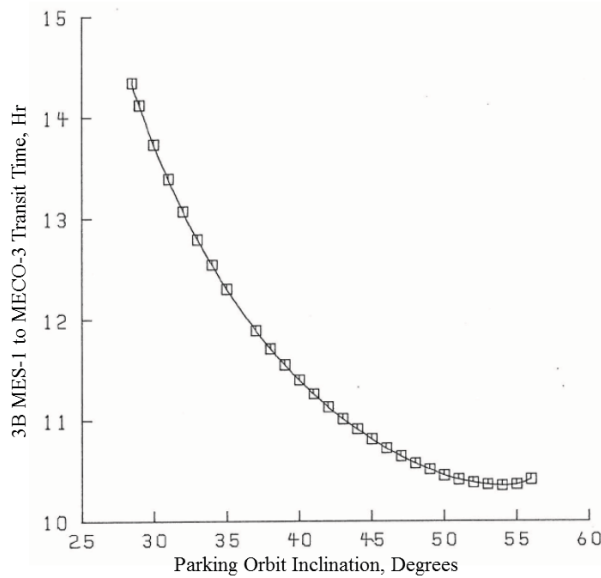


**Figure 14. Mission Elapse Time vs. Park Orbit Inclination for 3B Transfer.**

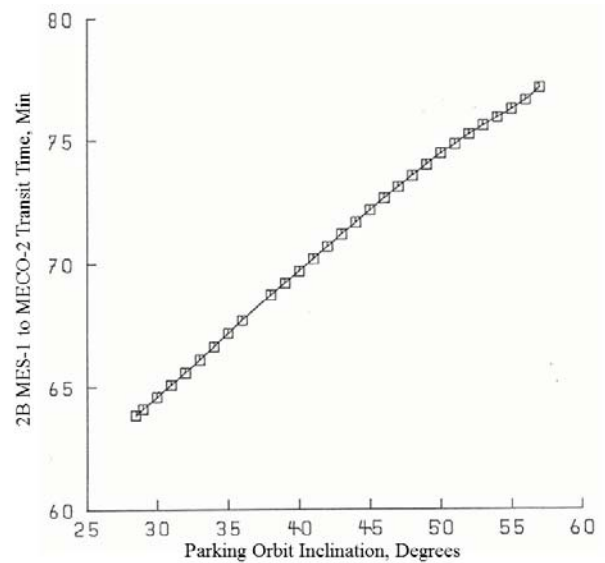


**Figure 15. Mission Elapse Time vs. Park Orbit Inclination for 2B Transfer.**

### C. Other consumables (electrical power, N<sub>2</sub>H<sub>4</sub>, He)

A major concern of the 3B transfer was the long MET (12 hrs at  $i = 37^\circ$ ), driven largely by the second transfer orbit. Additional electrical power would be necessary to keep the stage alive. The standard Shuttle/Centaur G battery complement was three 250 Amp-hr batteries. At a typical 80 Amp average current usage, they provided enough power for only 9 hours, short of the needs for a 3B Molniya transfer. One solution to this shortfall was to use two of the three optional 150 Amp-hr payload batteries available on the G vehicle. Though intended for the payload, mission peculiar hardware could have been added to use them for Centaur instead in order to accommodate the longer duration 3B mission. Table 4 shows the estimated power requirements for a 3B Molniya mission. Electrical power usage (per unit time) by Centaur was roughly equally split between avionics and fluid control, with the latter varying meaningfully depending on whether the propulsion system was in a coast, transient, or main burn phase.<sup>13</sup> Thus, duration was the primary driver of total power requirements. Using the standard complement of three Centaur batteries augmented by two payload batteries, a total 1050 Amp-hr was available to satisfy the calculated 943 Amp-hr required for a 3B mission starting from a  $37^\circ$  park orbit. The additional weight hit would be significant: 170 lbs of batteries and ~ 30 lb for miscellaneous power transfer unit hardware and harnessing.

**Table 4. Power Requirements for 3B Transfer**

		Total		Load	Required
	seconds	seconds	hours	(Amp)	(Amp-hr)
Coasts		43045	11.957	76.5	914.7
Transfer orbit 1	5361				
Transfer orbit 2	35884				
Post MECO-3	1800				
Burns		409	0.114	93.0	10.6
Burn 1	285				
Burn 2	98				
Burn 3	26				
Transients (3)		750	0.208	83.0	17.3
Total requirement		44204	12.279		942.6
Total capability of 3 Centaur + 2 payload batteries:					1050.0

Two other consumables were also evaluated: hydrazine (N<sub>2</sub>H<sub>4</sub>) and helium (He). The standard Molniya mission loading of N<sub>2</sub>H<sub>4</sub> monopropellant for the reaction control engines were 2 bottles (which included a 117 lb unallocated reserve). This was ample reserve to accommodate the additional 79 lb of N<sub>2</sub>H<sub>4</sub> required for Transfer Orbit 2 (Table 5 and Appendix D).<sup>5,7</sup> Regarding helium usage, the standard He pressurant loading were 2 large and 1 small bottle, for a total of 24 lb (which included a 5½ lb unallocated reserve). The additional He needed for Transfer Orbit 2 and Burn 3 usage was almost 9 lbs. This could have been accommodated by replacing the small He bottle with a large bottle, which would satisfy the He usage while still maintaining a small (~1¼ lb) margin (Table 5).<sup>3,5</sup> So the increased usage of both of these consumables could be accommodated with only modest system impacts. The additional net weight hit would be ~10 lbs (for the larger He tank).

**Table 5. Hydrazine and Helium Usage**

	N2H4	N2H4	He	He
	2 Burn	3 Burn	2 Burn	3 Burn
	(lb)	(lb)	(lb)	(lb)
Pre-MES-1 usage	44	44	1.60	1.60
Burn 1			7.34	7.34
Transfer orbit 1	79	79	0.25	0.25
Burn 2			8.73	8.73
Transfer orbit 2	0	79	0	0.25
Burn 3			0	8.73
Post last MECO	13	13	0.63	0.63
Collision, contamination avoid	49	49	0	0
Dispersions/residuals/errors	38	38	0	0
Unallocated reserve	117	38	5.45	1.27
Total	340	340	24.00	28.80
N2H4 bottle (170 lb)	2	2		
He bottle (large)			2	3
He bottle (small)			1	0

### V. Launch Windows

An analysis was done on the performance penalties associated with generating launch windows and deployment on later revolutions. This was done by having Centaur compensate for the orbit's nodal shift due to the Earth's rotation due to early or late launch, and/or the regression of the node ( $\Omega$ ) for late deployment. Figures 16 & 17 summarize 3B and 2B launch window performance penalties respectively. The maximum performance/zero penalty ( $y = 0$ ) reference point was an on-time launch ( $x = 0$ ) and deployment on the 5th orbit (revolution) of the Space Shuttle. All other launch times (either early or late) and later deployment revolutions resulted in a performance penalty due to the out of orbital plane yaw steering which had to be done to correct the  $\Omega$ . The ordinate axis was expressed in terms of change in pounds of propellant excess (PE), which was the additional Centaur propellant which had to be consumed to perform this nodal correction. Since the yaw steering constituted a loss in available performance, the ordinate was plotted as negative values. Performance losses were also calculated for two succeeding revolutions (6th and 7th). Each successive revolution had a performance loss due to LH<sub>2</sub> propellant boil-

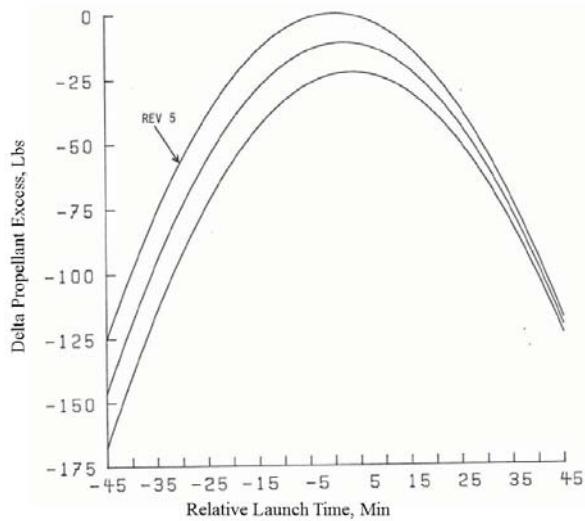


**Figure 16. Launch Window Performance Penalties for 3B Transfer.**

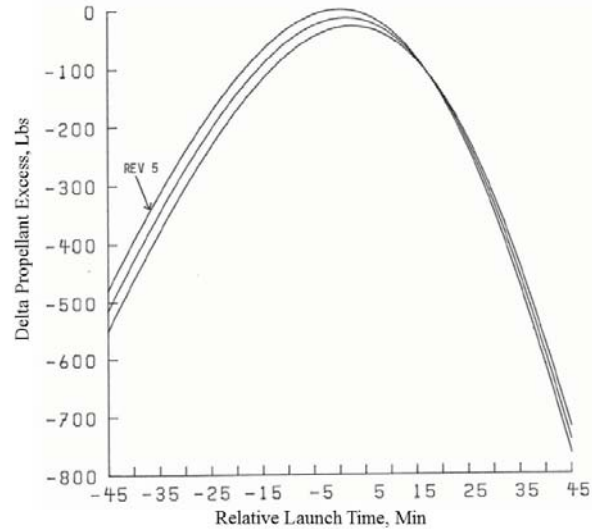


**Figure 17. Launch Window Performance Penalties for 2B Transfer.**

off (thus the vertical shift downward for each curve). The optimum of each revolution also shifted to a later time due to nodal regression. The park orbit inclinations used for the 3B and 2B cases were  $37^\circ$  and  $57^\circ$  respectively.

The 3B and 2B launch window performance penalty curves varied considerably. Comparing the ordinates, a 45 minute early launch with a revolution 7 deployment produced a  $\sim 170$  lb PE penalty for the 3B transfer, yet the penalty for the same conditions was  $\sim 550$  lbs of PE for a 2B transfer. If a Launch Time Reserve (LTR) of only 100 lbs was available, then the launch window using a 3B transfer could be as long as  $\sim 70$  minutes for a deployment on revolutions 5 through 7. For a 2B transfer, however, the same LTR would only enable a  $\sim 28$  minute window. The 3B and 2B LTR's for three fixed window lengths are shown in Table 6. For the same range of revolutions (5, 6, & 7), the longer the window, the more desirable the 3B transfer became. Example: the LTR for a 15 minute 2B window ( $\sim 48$  lbs) would be more than enough for a 30 minute 3B window ( $\sim 37$  lbs), whereas a 1 hr 2B window ( $\sim 320$  lbs) would be more than four times the LTR as a 1 hr 3B window ( $\sim 78$  lbs). The advantage of a 3B transfer was not just significantly better performance due to lower LTR propellant needed to be held in reserve, but also improved launch operations by increasing tolerance to launch delays, reducing the chance of scrubbing a launch.

To illustrate the launch window physics of 3B vs. 2B, Fig. 18 compares performance penalties for varying launch times for a single deployment revolution (rev 5). It will be shown that nodal change, like that of inclination, was solely a function of out of orbital plane thrust. Since it has been shown that the large out of plane yawing was

**Table 6. Launch Window Penalties for 3B and 2B Transfers.**

	Window Length (min)	PE Penalty (lb)	Window Opens (min)	Opening Rev	Window Closes (min)	Closing Rev
3 Burn	15	-26.3	-4.0	7	11.0	7
	30	-36.7	-11.5	7	18.5	7
	60	-77.7	-26.2	7	33.8	7
2 Burn	15	-47.7	-5.3	7	9.7	7
	30	-103.4	-13.4	7	16.6	7
	60	-320.4	-31.1	7	28.9	5

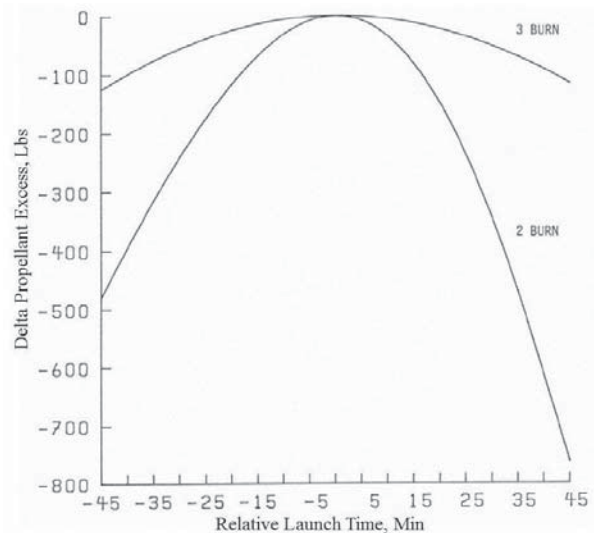


**Figure 18. Launch Window Performance Penalties for 3B vs. 2B Transfers (Rev 5 Only).**

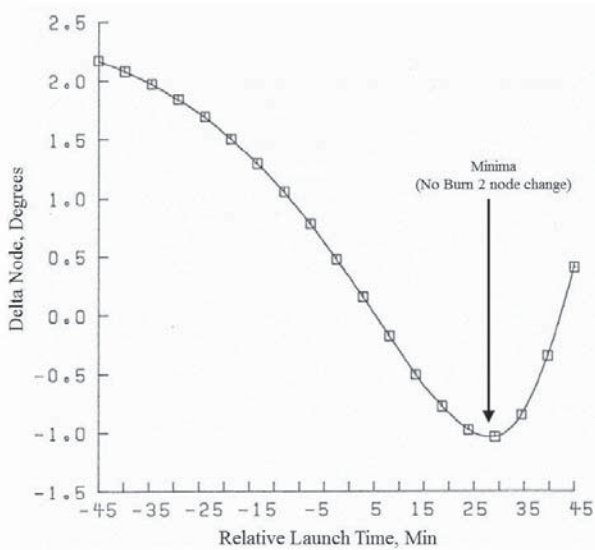


**Figure 19. Node Change in Launch Window During Burn 1 for 2B Transfer.**

performed more efficiently in a 3B transfer, it was expected that launch window penalties for 3B would be less severe than those of 2B (manifested by the significant difference between the curves in Fig. 18). To compare the relative ease of shifting  $\Omega$  between 3B and 2B transfers, first examine how much  $\Omega$  is changed by each burn. Figures 19 & 20 show 2B's  $\Delta\Omega$  vs. launch time for Burns 1 and 2 respectively. Figure 21 shows similar data for all three burns in the 3B transfer. The summation of  $\Omega$  changes for all burns at  $t = 0$  denotes the optimum amount of node change for an on-time launch. (Note: the total change in  $\Omega$  at  $t = 0$  is not zero, but rather the non-zero value which is optimum.) For any other launch time or deployment revolution (early or late with respect to the optimum), a different amount of  $\Omega$  change would take place at each burn. The difference in the sum of  $\Omega$  changes for any launch time/deployment rev combination with respect to the sum at  $t = 0/\text{rev } 5$  reflected the additional required out of plane yaw steering to correct the  $\Omega$ .

For the 2B transfer, most of the node correction was performed by Burn 2. This would be expected since out of plane thrusting is more efficient at low velocities (thus higher altitudes). The curve in Fig. 20 is almost linear with a negative slope, where early launches would need increased (easterly rotated) nodes and vice versa. At  $t = +27.4$  minutes, however, the curve passed through zero due to the geographic location at the equator. (The  $\Omega$  cannot be changed when the position is already at the node.) Around that location, the  $\Omega$  shift had to be done solely by Burn 1. This was manifested by the minima in Fig. 19 which corresponded to this point. Though barely visible, inflection points are present in Fig. 20 which corresponds to both points of zero  $\Omega$  change in Fig. 19. These are not due to the geographic position Burn 1, but rather the change in sign in optimal  $\Omega$  shift by Burn 1.

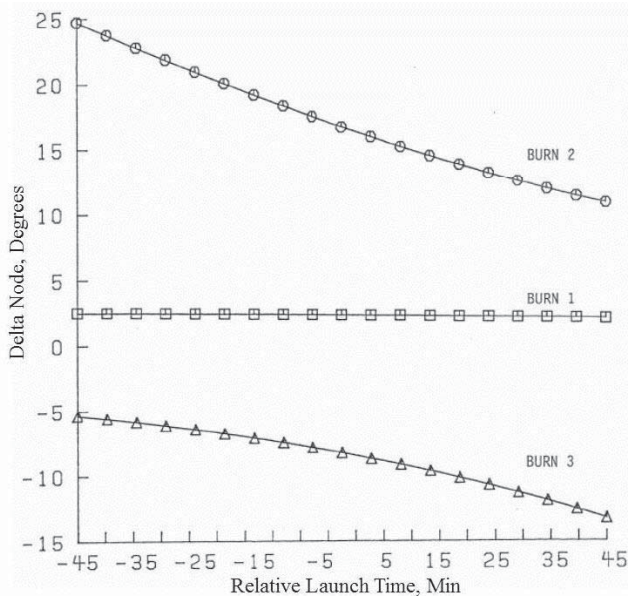


**Figure 21. Node Change in Launch Window During All Burns for 3B Transfer.**

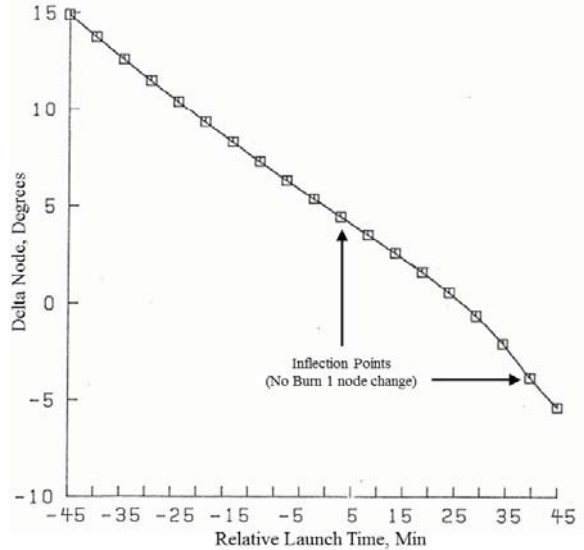


**Figure 20. Node Change in Launch Window During Burn 2 for 2B Transfer.**

For the 3B transfer (similar to 2B), most of the  $\Omega$  correction was done by the mostly out of plane Burns 2 & 3, with only a small amount ( $\sim 2\frac{1}{2}^\circ$ ) done by the in plane Burn 1 (Fig. 21). Similar to the earlier discussion, the amount of  $\Omega$  change was shared by Burns 2 & 3 in a more optimal way than 2B. For early launch, the  $\Omega$  was over-corrected (increased; easterly rotated) by Burn 2, then reduced modestly by Burn 3. For late launch, the  $\Omega$  was

under-corrected by Burn 2 with the node further corrected (decreased; westerly rotated) by Burn 3. Since neither Burn 2 nor 3 were located near the equator, Burn 1 did not fluctuate as it did in 2B. Also, since there were no zero  $\Omega$  change points throughout the window for any burn, there were no inflection points.

$$\frac{\partial \Omega}{\partial t} = \left[ \frac{r \sin(\theta + \omega)}{\sqrt{l\mu} \sin i} \right] W \quad (5)$$

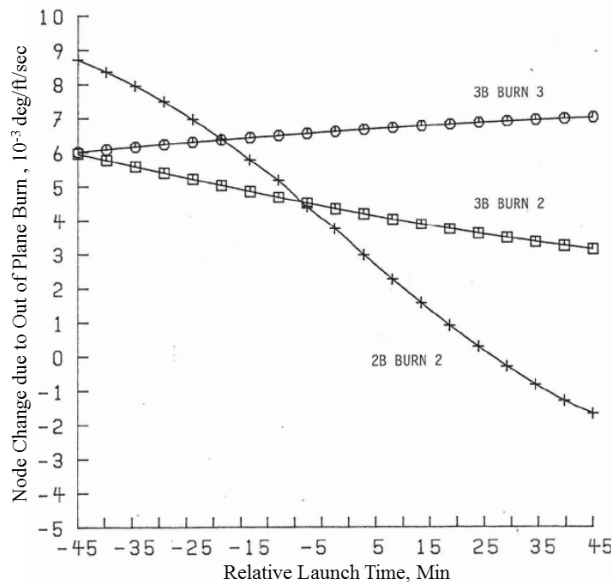


**Figure 22. Coefficients of Time Derivative of Node for Burns 2 & 3 for 3B Transfer and Burn 2 for 2B Transfer.**

To better understand why the trajectory optimization arrived at these solutions, the same approach used in the earlier discussion on orbital element changes is used here (employing a time derivative of an orbital element as a function of thrust components). Equation 5 is the time derivative for  $\Omega$  and is seen to be solely a function of out of orbital plane (yaw) thrusting.<sup>11</sup> It was plotted in Fig. 22 (analogous to the data in Table 3) using data from the launch window trajectories of Burns 2 & 3 for the 3B and 2B transfers. Over most of the opportunity, 2B was not as efficient in changing  $\Omega$  compared to 3B, as the 3B Burn 3 values exceeded  $6 \cdot 10^{-3}$  deg/ft/sec. For early launches, there was less of a difference between 3B's Burns 2 & 3. However, for very early launches ( $-45 < t \text{ (min)} < -25$ ), 2B had more favorable conditions with values exceeding  $9 \cdot 10^{-3}$  deg/ft/sec. Nevertheless, the benefit of splitting up the yaw over Burns 2 & 3 in 3B more than compensated for the slightly unfavorable orbital elements present in the early part of the window. In order to understand how each of the orbital elements effected Equation 5 throughout the windows, Fig. 23 - 26 show  $\theta$ ,  $\omega$ ,  $\sin(u)$ , and 'r' as functions of launch time for Burns 2 & 3, for the 3B and 2B transfers (argument of the latitude  $u = \theta + \omega$ ). The

inclination and semi latus rectum were fairly constant throughout the window. Note in Fig. 23, 3B's Burn 3 was plotted negatively to enable viewing on the same axis.

For the 2B transfer, the orbital elements for early launch were such that the nodal time derivative values were greater for 2B than those of the 3B transfers. Burn 2 for both 2B and 3B was greatly out of plane and positive, which enabled the  $\Omega$  to be moved move readily in an eastwardly direction to correct for early launch.  $\sin(u)$  and 'r' were greater for 2B than 3B, which enabled easier  $\Omega$  correction (i.e. greater Equation 5 values).

For late launch, however, the situation was quite different. Since  $\Omega$  had to be reduced (rotated westerly) relative to the node at  $t = 0$  for positive out-of-plane thrust angle,  $\theta$  had to be reduced greatly in order for the argument of the latitude to go negative (thus  $\sin(u)$  to go negative). This is apparent in Fig. 23 where  $\theta$  dramatically decreased, from  $128^\circ$  for on-time launch ( $t = 0$ ) to  $66^\circ$  for a 45 minute late launch. Since  $\omega$  was negative and close to the final Molniya value (Fig. 24), this large change in  $\theta$  drove the 'u' from  $36^\circ$  to  $-40^\circ$ , which drove  $\sin(u)$  from 0.59 to -0.63 (Fig. 25). The  $\theta$  change also greatly decreased 'r', because of the highly eccentric orbit ( $e = 0.715$ ). For every 5 minute delay in launch, the radius at which Burn 2 took place decreased by approximately 470 nmi at window opening and 445 nmi at window closing, and by ~950 nmi at mid-window. In total, the altitude decreased from a high of 14,740 nmi at window open to 1,270 nmi at window close (Fig. 26). As launch time became later, Burn 2 shifted toward node, crossing the equator, and then preceded the node (i.e. moved into the southern hemisphere). The combined effect of these changes was a large reduction in the time derivative of the  $\Omega$  for late launch, driving up the performance penalty for 2B transfer. While the combined changes in 'r' and  $\sin(u)$  drove Equation 5, it was primarily the decrease in 'r' which drove the time derivative of  $\Omega$  as can be seen by comparing the curves in Fig. 22 to Fig. 26. This also explains the severe asymmetry of the 2B curve in Fig. 18, where late launch was significantly more costly than early launch (-765 lb of PE vs. -480 lb of PE, respectively).

For the 3B transfer (unlike 2B) the  $\Omega$  change was shared by Burns 2 & 3 as was seen in the baseline case. Figure 23 shows that  $\theta$  remained almost constant throughout the launch window. (Note that Burn 3 was plotted with negative values to facilitate plotting both curves on the same axis.)  $\theta$  varied only  $9^\circ$  from early to late launch for

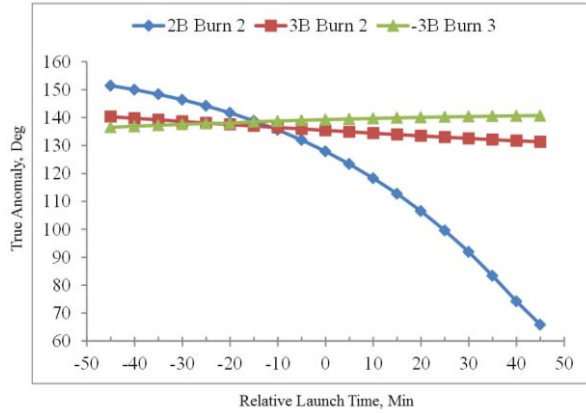


**Figure 23. True Anomaly Change in Launch Window During Burns 2&3 for 3B Transfer and Burn 2 for 2B Transfer.**

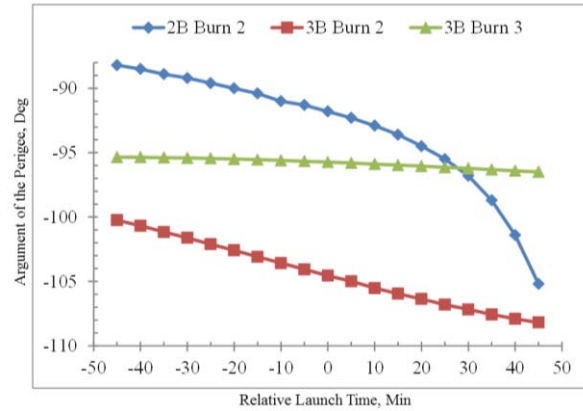


**Figure 24. Argument of the Perigee Change in Launch Window During Burns 2&3 for 3B Transfer and Burn 2 for 2B Transfer.**

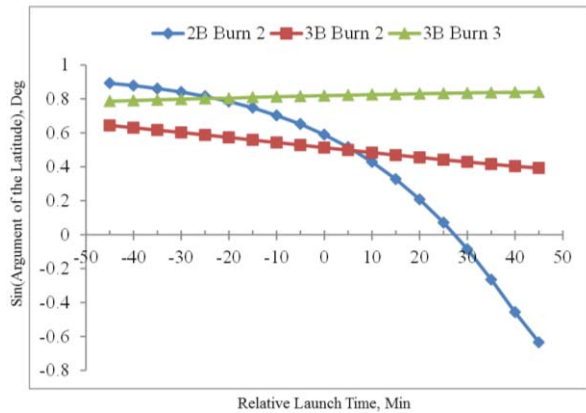


**Figure 25. Sin(Argument of the Latitude) Change in Launch Window During Burns 2&3 for 3B Transfer and Burn 2 for 2B Transfer.**

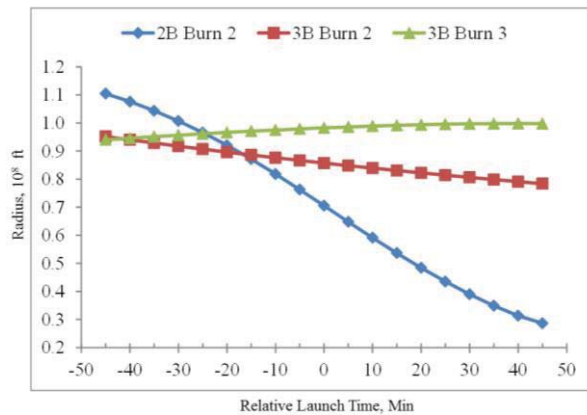


**Figure 26. Radius Change in Launch Window During Burns 2&3 for 3B Transfer and Burn 2 for 2B Transfer.**

Burn 2, and only  $4^\circ$  for Burn 3.  $\omega$  was similarly invariant, shifting less than  $8^\circ$  for Burn 2 and  $1^\circ$  for Burn 3 (Fig. 24). Thus  $\sin(u)$  was relatively invariant and of opposite slope for Burns 2 & 3, permitting flexibility in nodal correction (Fig. 25). The radius for 3B transfer gradually decreased for Burn 2 and gradually increased for Burn 3, but both were relatively high and relatively invariant when compared to the large altitude changes in Burn 2 in 2B (Fig. 26). Indeed, Burn 2 varied only 2,770 nmi over the entire  $1\frac{1}{2}$  hour opportunity. Burn 3 always took place at a greater altitude than Burn 2 and vacillated even less. This permitted the change in  $\Omega$  to be optimally distributed over Burns 2 and 3. Since the out-of-plane component of Burn 3 was negative (opposite of the angular momentum vector), the  $\Omega$  could readily be moved westerly for late launches. So for the 3B transfer, a considerable amount of node change could be done over a widespread stretch of launch time and not result in a greatly diminished time derivative of node change as in 2B.

In summary, whether the goal is a longer window, smaller LTR, more deployment revolutions, or a combination of all three, 3B was significantly superior to 2B. For heavy payloads, where the LTR might be limited, this could mean the difference between a generous launch/deployment period with adaptability to ground operation delays, and a constricted launch opportunity inflexible to obstacles impeding launch.

## VI. Ground Tracks

Ground tracks were calculated for 2B and 3B transfers using the orbit/trajectory visualization software KPLOT from the NASA Jet Propulsion Laboratory based on results from DUKSUP.<sup>14</sup> This analysis included burn and coast phases as well as their variation within a 90 minute launch window. The ground track of the nominal (i.e. on-time) 2B transfer is shown in Fig. 27. The longitudinal position was largely a function of the parking orbit state vector and deployment revolution. Thus for the standard park orbit ( $i = 57^\circ$ ) and deployment revolution 5, Burn 1 took place halfway between South Africa and Antarctica. The long Burn 1 arc in LEO was located out of range of any ground tracking station and would necessitate one of two coverage options: the use of two Advanced Range Instrumentation Aircraft (ARIA) or the Tracking and Data Relay Satellite System (TDRSS) to secure telemetric data of the burns (or at least MES and MECO). The 2B ground track then passed through the southern Indian Ocean, skirting the western coast of Australia, through the Indonesian archipelago, passing southeast of the Philippines, culminating south of Japan where the Burn 2 ground track appeared as a short segment. Burn 2 should have been visible from the Guam Tracking Station (GTS (GWM)).

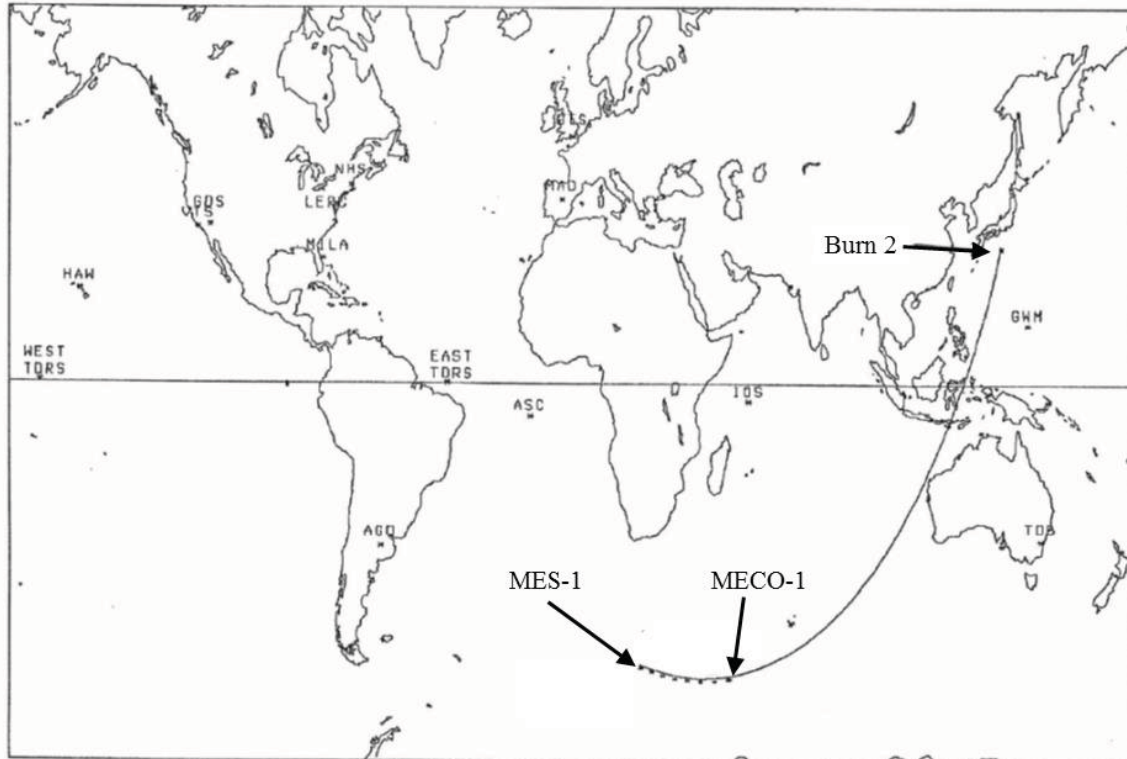


**Figure 27. Ground Track of 2B Transfer.**

The ground track of the nominal 3B transfer is shown in Fig. 28. For the park orbit ( $i = 37^\circ$ ) and deployment revolution 5, Burn 1 took place between the eastern South American coast and South Africa. As with the 2B transfer, the long Burn 1 arc in LEO was located out of range of any ground tracking station and would also have necessitated either two ARIA aircraft or TDRSS. Following Burn 1, the 3B ground track then skirted the South African coastline and diagonally bisected (southwest to northeast) the Indian Ocean. Burn 2 appeared as a short segment over Burma, but because of its high altitude, it should have been visible to both Diego Garcia Station (DGS) (i.e. Indian Ocean Station (IOS)) and GTS. The ground track then moved north and slightly westward (due to its decreasing Earth-relative speed as it approached apogee), crossing over China and Russia. Following apogee, the track proceeded in a due south direction until Burn 3 took place between the Areal Sea and Lake Balkash in Kazakhstan. Again, due to its high altitude, Burn 3 should have been visible to ground stations in this hemisphere, including Telemetry & Command Station (TCS) (i.e. RAF Oakhanger (England) Tracking Station (OTS)).

There was one primary difference between 3B and 2B ascent profiles relative to the Earth. Unlike the 2B transfer, 3B's Burn 1 passed through the center of the South Atlantic Anomaly (Fig. 29), a region of the Van Allen Radiation Belt in space which has an altitude as low as 108 nmi.<sup>15</sup> Proton ( $>50$  MeV) fluxes in excess of  $1000/(\text{cm}^2 \text{ sec MeV})$  could be experienced during Burn 1.<sup>15</sup> Because of this, assessments on the tolerances of both the Centaur stage and spacecraft avionics to this higher radiation environment would be necessary.

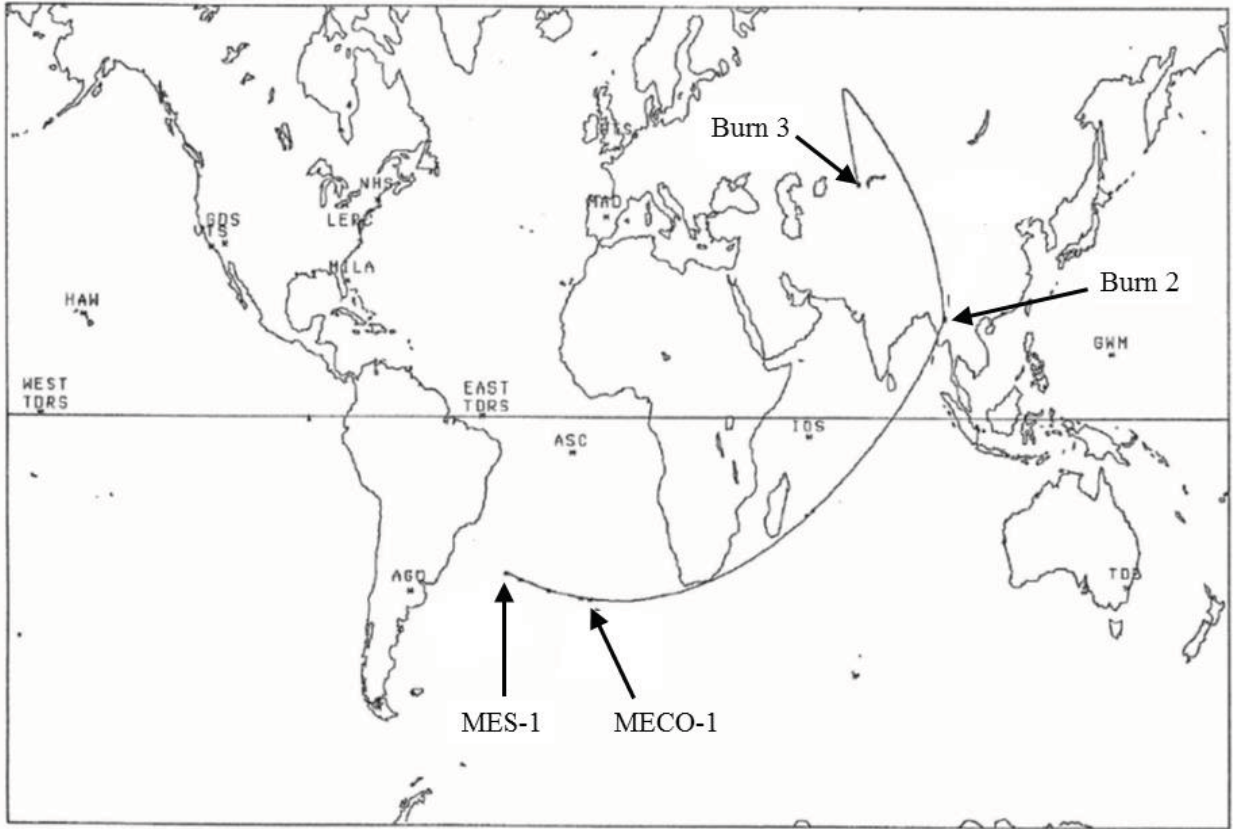


Figure 28. Ground Track of 3B Transfer.

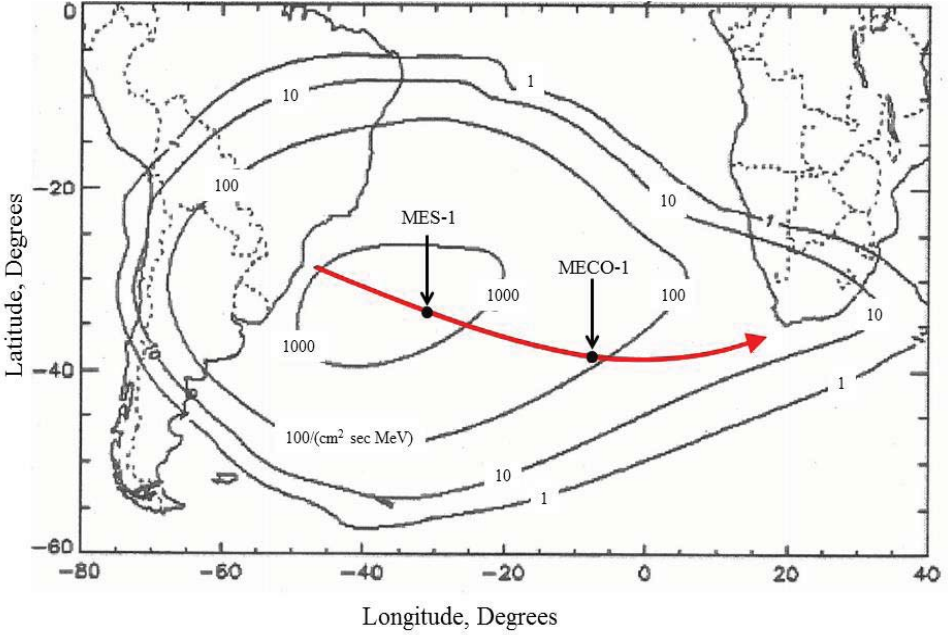
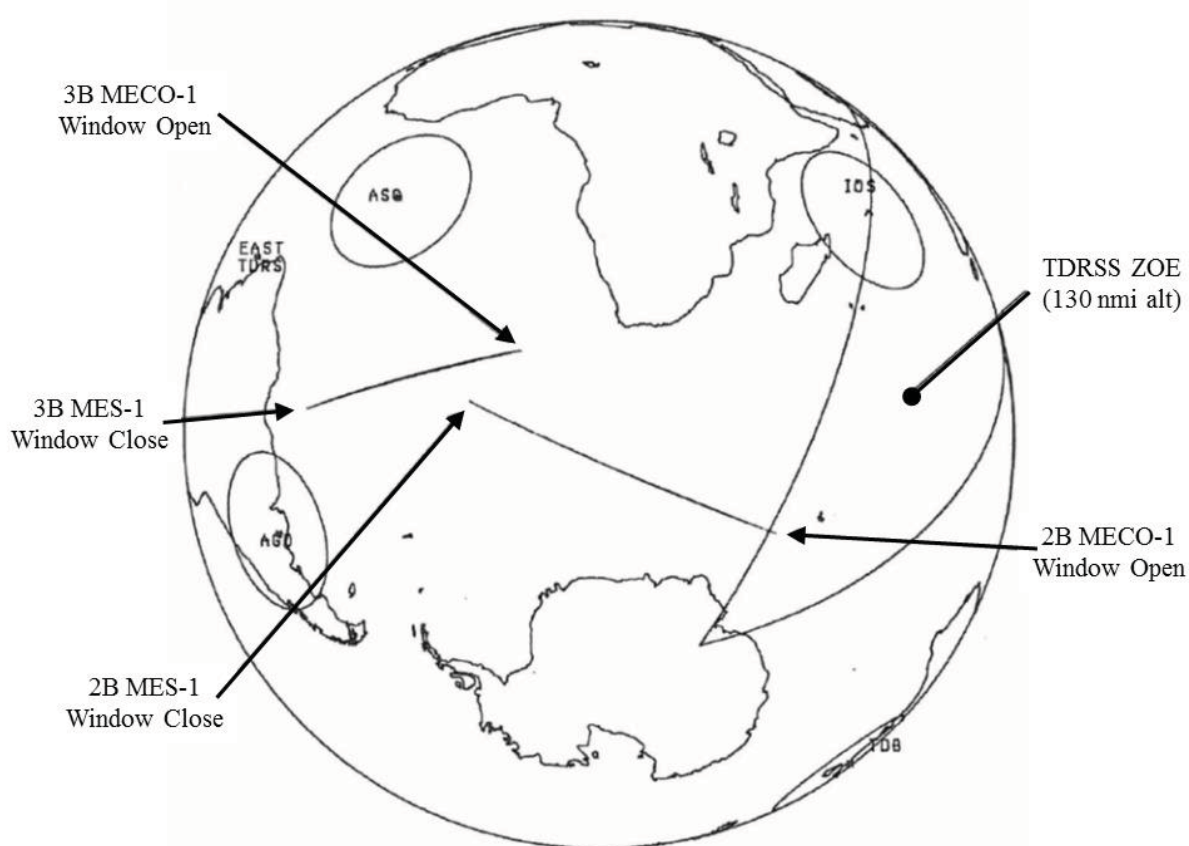


Figure 29. 3B Transfer Burn 1 Transit Through South Atlantic Anomaly.





**Figure 30. Burn 1 Ground Tracks for 3B and 2B Transfers Through Launch Window.**

The range of ground tracks for Burn 1 for both 2B and 3B as they varied throughout a 90 minute launch window are shown in Fig. 30. In both 2B and 3B transfers, the western-most start of the Burn 1 ground track was MES at window close (i.e. 45 minute late launch), while the eastern-most end of the Burn 1 ground track was MECO at window open (i.e. 45 minute early launch). The burns throughout the windows were coincident on the same arc, differing only in start and stop points. The nominal (on time) burn arcs were located in the center of the arcs shown in Fig. 30. All ground tracks shared the same tracking limitations as the mid-window (on time) ascents. Note however that MECO-1 for 2B at the opening of the launch window intruded slightly into the TDRSS Zone of Exclusion for that altitude. Because of the wide range of ground tracks through the window, additional ARIA might have been necessary for adequate coverage of the first burn.

The range of ground tracks for Burns 2 & 3 for both 2B and 3B throughout a 90 minute launch window are shown in Fig. 31. Due to the shortness of the burns, most of the ground tracks appeared as short segments or dots (i.e. MES and MECO were almost indistinguishable). Their range from launch window open to close, however, was considerable compared to their burn arcs. 2B's Burn 2 varied the most, from the west coast of Australia at window close to the Sea of Okhotsk north of Japan at window open. Recalling the earlier discussion on the variation of 'r' and  $\theta$  within the window (which drove the wide change in latitude), TDRSS support would be mandatory for 2B's Burn 2 since ARIA would not have been able to accommodate such a span of ground tracks. Also, given the relatively low altitude at window close, GTS would not likely be visible. 3B's Burns 2 & 3 were not as dispersed as Burn 2 of 2B's for the same reason as discussed earlier regarding out of plane yaw. 3B's Burn 2 ranged from the Bay of Bengal at window close to central China at window open. 3B's Burn 3 ranged from east of the Areal Sea at window close to south of Lake Balkash at window open, all within Kazakhstan. As with Burn 1, the nominal (on time) burn arcs were located in the center of the arcs shown in Fig. 31, though Burn 2 of 2B was more geographically offset (as shown). All burns (except 2B's Burn 2 late launch) were expected to be similarly visible to ground stations as the mid-window (on time) ascents because of their high altitude.

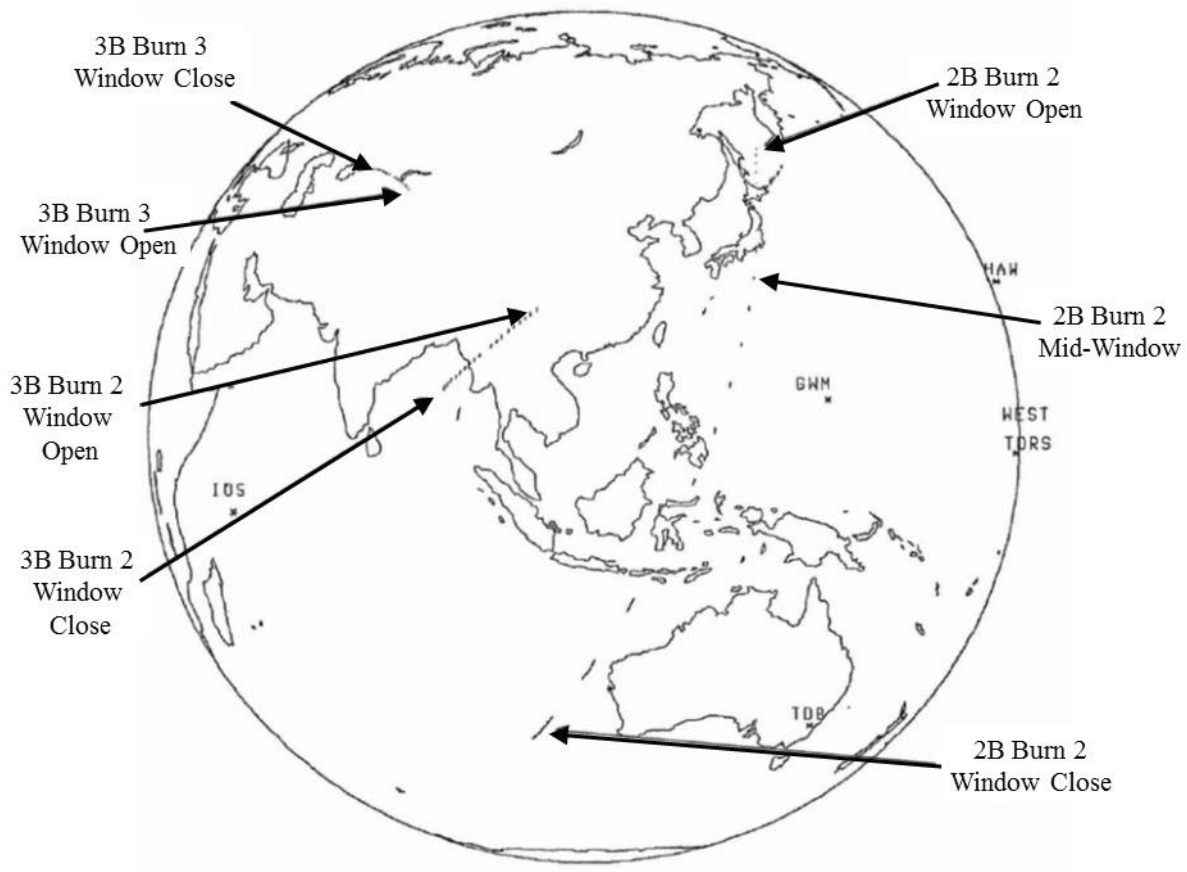


**Figure 31. Burns 2 & 3 Ground Tracks for 3B and 2B Transfers Through Launch Window.**

In summary, both 2B and 3B would require similar tracking assets (ARIA or TDRSS) for Burn 1. For the 2B transfer, Burn 2 would need TDRSS for a 90 minute launch window. Only with a significantly shortened window would Burn 2 be visible from a station such as GTS. For the 3B transfer, Burns 2 & 3 should be visible from various ground stations throughout a 90 minute launch window. This is despite the considerable differences in geographic over-flight locations. The 3B transfer, however, did have an additional operational concern pertaining to flight through the center of the South Atlantic Anomaly during Burn 1.

## **VII. Relevance to Future Missions**

While the Shuttle/Centaur G vehicle never flew, this analysis has a few of potential applications to future missions. As was mentioned, all ELVs' lift capabilities are degraded as launch azimuth is decreased from 90° due East. Should another booster & upper stage combination find itself in a similar situation in attempting to perform a performance-demanding Molniya (or similar) mission, most of the orbital mechanics and engineering analysis contained in this study should still be relevant. Another application pertains to national security interests, which might find interesting the impacts of on-orbit loitering analogous to the Space Shuttle's multiple revolution operations prior to upper stage/payload deployment. Further, a transfer such as 3B to Molniya could help "camouflage" the transfer orbit. Lastly, it is believed by the author that this paper represents one of the few documents explaining the physics of finite launch windows combined with multiple revolution space operations for a generic Molniya mission in the open literature. Thus, this material should be useful for certain future applications.

## VIII. Conclusions

While it has been almost 30 years since the joint NASA-USAF Shuttle/Centaur program developed stages for performance-demanding missions such as Molniya orbit, much of the analytical work was never documented. The unconventional three orbital burn transfer to Molniya orbit was one of those works. This alternate transfer was pursued primarily to mitigate a major concern of the time pertaining to propellant slosh-dynamics during deployment from the Shuttle cargo bay. Today, however, the performance and orbital mechanics of this transfer should be of interest academically, and also may have applications for future national security missions.

The most unusual characteristic of the three burn (3B) transfer was that the total energy of its second transfer orbit was significantly greater than that of the final orbit. This was unusual among orbit transfers, which typically are monotonically increasing in orbital energy. But it was nevertheless optimal because of how the optimization performed the out of plane maneuvers to satisfy angular orbital element ( $i$  and  $\omega$ ) requirements in a more efficient way than could be done in the two burn (2B) transfer. Thus the 3B transfer with comparable performance to the 2B transfer existed because it was advantageous to increase 'a' and  $R_p$  beyond their target values, only to subtract them back out in order to split up and perform the inclination and  $\omega$  changes in more favorable orbital element spaces.

The Centaur with fully loaded propellant tanks could be flown from a  $37^\circ$  inclination low Earth parking orbit via a 3B transfer to achieve Molniya orbit with comparable performance to the base-lined 2B transfer (9,545 lb vs. 9,552 lb of separated spacecraft weight respectively) which started from a  $57^\circ$  inclined orbit and required a 40% propellant offload. There was a significant reduction in the need for propellant launch time reserve for a one hour window: only 78 lb for the 3B transfer vs. 320 lb for the 2B transfer. This also meant that longer launch windows over more orbital revolutions could be done for the same amount of propellant reserve. These performance results were due to 3B's ability to more optimally distribute the out-of-orbital plane steering changes in inclination,  $\omega$ , and  $\Omega$  over three burns rather than just two. While the 3B vs. 2B ground tracks varied considerably, there was no practical difference in ground tracking station or airborne assets needed to secure telemetric data, even though the geometric locations of the burns varied considerably. One potential issue was that the first burn of the 3B transfer would traverse the most intense region of the South Atlantic Anomaly, requiring an assessment of the impacts of this high radiation environment on both Centaur and payload. The 3B transfer did entail a significant adverse increase in total mission time compared to 2B (12 hrs vs. 1¼ hrs). However, the longer transfer time could be accommodated by using existing (though optional) payload batteries (necessitating a significant performance hit), using unallocated reserves in hydrazine RCS propellant, and swapping helium pressurant bottles.

**Table 7. Summary Figures of Merit for 3B vs. 2B Transfers**

	3 Burn	2 Burn
Propellant Loading	Full tanks	40% Offload
Payload (lb)	9,545	9,552
Mission Elapse Time (hr)	12	1¼
Launch Window (1 hr) (lb PE)	78	320
Ground Tracks (nominal)	SAA intrusion	Managible
Ground Tracks (window)	Manageble	Burn 2 span
Vehicle Modifications	Battery harness; He bottle swap; ~210 lb total hit	None

Finally, it is important to acknowledge the satisfying of the primary objective of the study: to establish the validity of the hypothesis that the 3B transfer could perform the Molniya mission with comparable performance while fully loading the propellant tanks on Centaur. As is illustrated in the summary Table 7, a reasonable case could be made that (all issues considered) the 3B transfer would have been preferable to the baselined 2B transfer.

**Appendix A**  
3 Burn and 2 Burn Propellant Tanking Information  
 (All modeling taken from Mini-Colt. <sup>3</sup>)

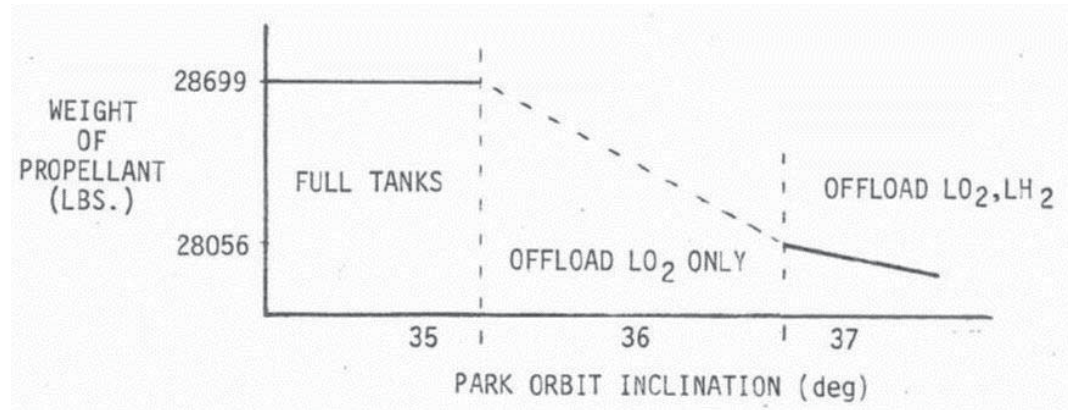
For 3 Burn:

WPMAX = maximum allowable main impulse propellant  
 = total tankable – settlings – residuals – CVR for 12 hr mission – FPR (from full tanked mission)  
 = 30,366 – 806 – 413 – 188 – 260  
 = 28,699 lbs

Inclination where initial weight = weight limit defined point where offloading of LO<sub>2</sub> began (at i = ~35.75°)  
 Inclination where offloading of both LO<sub>2</sub> and LH<sub>2</sub> defined by:

$$\frac{(LO_2)_{\max} x}{(LH_2)_{\max}} = 6.0 = \frac{25,075}{4,072} x \text{ yields } x = 643 \text{ lbs.}$$

Thus 28,699 – 643 = 28,056 lbs at i = ~36.75°



For 2 Burn:

WPMAX = 30,366 – 573 – 413 – 188 – 260 = 28,932 lbs

$$\frac{25,222 - x}{4,158} = 6.0 \text{ yields } x = 274 \text{ lbs}$$

At 28,932 – 274 = 28,658 lbs. began offloading both LO<sub>2</sub>, LH<sub>2</sub>. This occurred at 37° > i > 38°.

FPR = Flight Performance Reserve  
 CVR = Centaur Vehicle Reserve

**Appendix B**  
RL10 Propulsion System Modeling

In fully tanked region of inclinations, the RL10A-3-3B engine characteristics are:

For 3 Burn:

$$O/F = \frac{25,075}{4,072} = 6.1579$$

Thrust = 30,130.74 lbs  
WTFLOW = 68.6937 lbs/sec

For 2 Burn:

$$O/F = \frac{25,222}{4,158} = 6.0659$$

Thrust = 30,130.74 lbs  
WTFLOW = 68.6937 lbs/sec

In offloaded region of inclinations:

3 Burn and 2 Burn:

O/F = 6.0  
Thrust = 30,036.0 lbs  
WTFLOW = 68.25 lbs/sec

### Appendix C

#### Net Payload Calculations

(All constants were taken from mini-Colt. <sup>3</sup>)

“wet Centaur” = dry Centaur + FPR + CVR + residuals

For full tanks, both 3 Burn and 2 Burn:

$$\begin{aligned} \text{Payload} &= \text{burnout weight} - \text{wet Centaur} \\ &= \text{burnout weight} - (\text{dry Centaur} + \text{FPR} + \text{CVR} + \text{residuals}) \\ &= \text{WF} - (6,574 + 260 + 188 + 53) \\ &= \text{WF} - 7,533 \end{aligned}$$

For offloaded region, both 3 Burn and 2 Burn:

$$\begin{aligned} \text{Payload} &= \text{WF} - (6,574 + 260 + 454 + 550) \\ &= \text{WF} - 7,838 \end{aligned}$$

WF = “burnout weight”

FPR = Flight Performance Reserve

CVR = Centaur Vehicle Reserve

### Appendix D

#### LH<sub>2</sub> Boiloff Modeling and Reaction Control System (RCS)

For 3 Burn:

LH<sub>2</sub> boiloff rate was extrapolated from geosynchronous (GEO) mission

Using 19 lbs/5.08 hr:

1st transfer orbit coast phase vent = 8.2 lbs.

2nd transfer orbit coast phase vent = 44.5 lbs

For fully tanked mission

N<sub>2</sub>H<sub>4</sub> pre MES-1 = pre MES-1 for fully tanked mission (GEO)

N<sub>2</sub>H<sub>4</sub> pre MES-2 and pre MES-3 = pre MES-2 for GEO

N<sub>2</sub>H<sub>4</sub> post MECO-2 and post MECO-3 = post MECO-2 for offloaded mission (Molniya)

For offloaded region:

N <sub>2</sub> H <sub>4</sub> pre MES-1	= pre MES-1 for fully tanked mission (GEO)
N <sub>2</sub> H <sub>4</sub> pre MES-2	= pre MES-2 for GEO
N <sub>2</sub> H <sub>4</sub> pre MES-3	= pre MES-3 for Molniya

For 2 Burn:

All fuel ventings and RCS propellants were kept at the same values given in mini-Colt 6 for Molniya mission. Offloaded and fully tanked regions were modeled the same.

**Appendix E**

Approximation by Drop Masses

Masses which are dropped at the end of Transfer Orbits 1 and 2 (M<sub>D1</sub> and M<sub>D2</sub> respectively) could be used to approximate the pre-chill, pre-start, and start-up transients which, while significant consumers of propellant, contributed little ΔV for the mission. Using fixed ΔVs for all three burns (taken from integrated computer runs for park orbit at i = 37°), the mass ratios (L<sub>2</sub> and L<sub>3</sub>) for Burns 2 & 3 respectively were given by:

$$L_2 = \frac{M_{prop\ 2} + (M_{PL} + M_{ST})(L_3 - 1) + M_{D2} + M_{PL} + M_{ST}}{(M_{PL} + M_{ST})(L_3 - 1) + M_{D2} + M_{PL} + M_{ST}}$$

$$L_3 = \frac{M_{prop\ 3} + M_{PL} + M_{ST}}{M_{PL} + M_{ST}}$$

Substituting these expressions into the rocket equation representing the total ΔV<sub>T</sub> of all three burns resulted in the expression (where M<sub>T</sub> is total initial mass which is a constant, ΔV<sub>T</sub> = 13,502.5 ft/sec = constant, and RL10 I<sub>sp</sub> = 440.1 sec from Appendix B):

$$L_2 L_3 (M_{PL} + M_{ST}) + L_2 M_{D2} + M_{D1} = L_2 L_3 M_T e^{-\Delta V_T / g_c I_{sp}}$$

Differentiating with respect to each drop mass separately yielded (for fixed ΔV's from integrated runs):

$$\frac{\partial M_{PL}}{\partial M_{D1}} = \frac{-1}{L_2 L_3} = -0.67$$

$$\frac{\partial M_{PL}}{\partial M_{D2}} = \frac{-1}{L_3} = -0.9$$

Where:

M<sub>PL</sub> is payload mass

M<sub>D1</sub> and M<sub>D2</sub> are drop masses (losses) at the end of transfer orbits 1 and 2 respectively

L<sub>2</sub> and L<sub>3</sub> are mass ratios for Burns 2 and 3 respectively

M<sub>prop</sub> is the propellant mass for each burn

For vanishing 3B transfer at park orbit with i = 57°, these partials were in the limit -0.9 and -1.0 respectively.

## Acknowledgments

The author would like to thank and acknowledge the considerable body of analytic research into the three burn problem by Dr. Keith Zondervon of The Aerospace Corporation, without which this analysis could not have been possible. Special thanks to Mr. Frank Spurlock (ret.) of the NASA Lewis Research Center for his guidance and use of his renowned computer program DUKSUP, which was the generator of the data contained in this paper. Finally, special gratitude is extended to Colonel William Files, USAF, Ret. (Space Division) for the extraordinary opportunity to work on one of this nation's finest launch vehicle development programs: Shuttle/Centaur.

## References

- 
- <sup>1</sup> Stofan, A. J., "A High Energy Stage for the National Space Transportation System", NASA TM 83795, 1984.
  - <sup>2</sup> "Shuttle/Centaur Program", General Dynamics Convair Division, San Diego, CA, 1983.
  - <sup>3</sup> Williams, C. H., "Generic Shuttle/Centaur G Vehicle/CISS Configuration, Weight, and Performance Baseline and Status" ("mini-Colt"), USAF Space Division Detachment OLAC at NASA Lewis Research Center, issue No. 6, Cleveland, OH, Sept. 1984.
  - <sup>4</sup> "Centaur Vehicle Simulation Data Book", General Dynamics Convair, Report No. GDC-SP-84-002, San Diego, CA, Mar 1984.
  - <sup>5</sup> "Shuttle/Centaur G Level III/IV Critical Design Review at LeRC", General Dynamics Space Systems Division, San Diego, CA, Oct 1984.
  - <sup>6</sup> "Centaur Vehicle Simulation Data Book (G Configuration)", General Dynamics Space Systems Division, Report No. GDSS-SSC-85-005, Contract NAS3-22901, San Diego, CA, May 1985.
  - <sup>7</sup> "Shuttle/Centaur G Configuration, Performance, and Weight Status Report" ("Colt"), General Dynamics Space Systems Division, Report No. GDSS-SSC-85-006-2, Contract NAS3-3322, San Diego, CA, Oct 1985.
  - <sup>8</sup> Zondervan, K. P., "Optimal Low Thrust, Three Burn Orbit Transfers with Large Plane Changes", PhD Thesis, California Institute of Technology, Pasadena, CA, 1983.
  - <sup>9</sup> Spurlock, O.F., Teren F., "Optimum Launch Trajectories for the ATS-E Mission", NASA TM X-52836, NASA Lewis Research Center, July 1970.
  - <sup>10</sup> Spurlock, O. F., Williams, C.H., "DUKSUP: A Computer Program for High Thrust Launch Vehicle Trajectory Design & Optimization", AIAA Propulsion and Energy Forum and Exposition 2014: 50th AIAA/ASME/SAE/ASEE Joint Propulsion Conference, American Institute of Aeronautics and Astronautics, pre-print, Control ID#: 1943459, Cleveland, OH, July 2014.
  - <sup>11</sup> Dobson, W.F., Huff, V.N., Zimmerman, A. V., "Elements and Parameters of the Osculating Orbit and Their Derivatives", NASA Technical Note D-1106, NASA Lewis Research Center, Jan 1962.
  - <sup>12</sup> Labuszewski, T.E., "ETR STS Payload Capability vs. Inclination for "Centaur Type" Missions", Internal letter, Rockwell International, Satellite Systems Division, Downey, CA, 30 Oct 1984.
  - <sup>13</sup> Hill, T. J., "Proposed Change to G-Generic Centaur Power Requirements", NASA LeRC Engineering Review Board Request data package, ERB No. 6342-70, Nov 1985.
  - <sup>14</sup> Schlaifer, R. S., Skinner, D. L., "KPLOT Users' Manual", NASA Jet Propulsion Lab, Release 1, with JPL correspondence (Diehl, R.) Jan 1984.
  - <sup>15</sup> South Atlantic Anomaly intensity map, [http://www.estec.esa.nl/wmwww/wma/rad\\_env.html](http://www.estec.esa.nl/wmwww/wma/rad_env.html)